

THESIS FOR DEGREE OF DOCTOR IN PHILOSOPHY

**Assessment of novel applications for  
nano-porous thermal insulation in district  
heating pipes and building walls**

Axel Berge

Division of Building Technology  
Department of Civil and Environmental Engineering  
CHALMERS UNIVERSITY OF TECHNOLOGY  
Göteborg, Sweden, 2016

Assessment of novel applications for nano-porous thermal insulation in district heating pipes and building walls

AXEL BERGE  
ISBN 978-91-7597-343-2

©AXEL BERGE, 2016.

Doktorsavhandling vid Chalmers Tekniska Högskola  
Ny serie nr: 4024  
ISSN: 0346-718X

Department of Civil and Environmental Engineering  
Division of Building Technology  
Chalmers University of Technology  
SE-412 96 Göteborg  
Sweden  
Telephone +46 (0)31-772 1000  
[www.chalmers.se](http://www.chalmers.se)

Cover: Bendable vacuum insulation panel for pipes (Chapter 3). (Photo: Nina Zanders)

Printed by Chalmers Reproservice  
Göteborg, Sweden 2016

Assessment of novel applications for nano-porous thermal insulation in district heating pipes and building walls

AXEL BERGE

Division of Building Technology

Department of Civil and Environmental Engineering

Chalmers University of Technology

## Abstract

In nano-porous thermal insulation there is a strong relation between the pressure and the thermal conductivity, even at pressures close to atmospheric pressure. This thesis presents research on applications of nano-porous insulation in hybrid insulation district heating pipes and in building walls.

A concept of hybrid insulation district heating pipes has been investigated where the innermost layers of insulation consists of nano-porous insulation and the outer layers consists of polyurethane foam insulation. The concept has been investigated through a mix of laboratory measurements, field measurements and simulations. The presented research indicates that vacuum insulation panels (VIPs) can be used in district heating pipes to reduce the heat losses. For the evaluated configurations the heat losses were reduced by a magnitude of 30%. The heat losses from the supply pipe in a twin pipe were reduced by 50%. The two main considerations with using vacuum panels in district heating pipes are the thermal bridges and the long term performance. It is shown that the position of the thermal bridges in the panels has a large effect on the thermal performance of the twin pipes and the results indicate a preferred configuration to minimize heat loss. The thesis presents a model to evaluate the long term performance of the VIPs through temperature measurements. After three years of field measurements on pipes connected to a district heating network with temperatures up to 90°C, there is no sign of any uncontrolled deterioration of the VIPs.

Results from the investigation show that the use of aerogel can reduce the thickness of a load bearing stud wall with 40% compared to the use of conventional insulation. If done wrong, this can lead to some new consideration regarding mold growth risk. The fact that the thermal conductivity of nano-porous insulation is strongly influenced by the pressure in the pore gas can be used to create variable insulation, where the thermal properties of the insulation is changed to match the current circumstances. By putting the insulation in a diffusion tight bag, connected to a vacuum pump, the pressure in the material can be changed and thereby the thermal conductivity. The pressure was varied in a fumed silica and an aerogel blanket sample between 1 kPa and atmospheric pressure, which gave a variation in the thermal conductivity of 1.5 for the aerogel blanket and 3 for the fumed silica. Transient measurements during evacuation and refilling show that the thermal performance will be influenced by some transient effects, such as influence from the temperature of the inserted air, but the time scale is too small to have any large effect on the energy performance. When the variation is used in simulations of the energy use for an office building, an interesting result is that a variable construction gave a higher optimum U-value, corresponding to thinner walls.



## List of publications

The thesis is based on the following publications, referred to in the text by Roman numerals I-VII. The publications are divided into two themes.

**Theme 1:** Hybrid insulation district heating pipes.

- I Explorative study of the thermal performance of superinsulation in district heating pipes (2016) Submitted to *Energy and Buildings*.  
Co-authors: Bijan Adl-Zarrabi.
- II Assessing the thermal performance of district heating twin pipes with vacuum insulation panels (2015) *Energy Procedia*, Vol. 78 pp. 382-387.  
Co-authors: Bijan Adl-Zarrabi, Carl-Eric Hagentoft.
- III Field measurements on a district heating pipe with vacuum insulation panels (2016) *Renewable Energy*, Vol. 87(3) pp. 1130-1138.  
Co-authors: Carl-Eric Hagentoft, Bijan Adl-Zarrabi.
- IV Finite element simulations of the thermal performance for district heating pipes with vacuum insulation panels (2016) Submitted to *Energy and Buildings*.  
Co-authors: Bijan Adl-Zarrabi, Carl-Eric Hagentoft, Paula Wahlgren.

**Theme 2:** Nano-porous insulation in building walls.

- V Wooden stud walls with aerogel thermal insulation (2013) Buildings XII Conference, Clearwater, USA.  
Co-authors: Carl-Eric Hagentoft, Paula Wahlgren.
- VI Changing internal pressure to achieve variable thermal conductivity in thermal insulation (2015) Advanced Building Skins Conference, Graz, Austria.  
Co-authors: Carl-Eric Hagentoft, Paula Wahlgren, Bijan Adl-Zarrabi.
- VII Effect from a variable U-value in adaptive building components with controlled internal air pressure (2015) *Energy Procedia*, Vol. 78 pp. 376-381.  
Co-authors: Carl-Eric Hagentoft, Paula Wahlgren, Bijan Adl-Zarrabi.

## Other publications

- Johansson, P., Adl-Zarrabi B. & Berge, A. (2015) Long-term performance of vacuum insulations panels in buildings and building systems. *IVIS2015 12th International vacuum insulation symposium*, China.
- Johansson, P., Adl-Zarrabi B. & Berge, A. (2015) Evaluation of long-term performance of VIPs. *Energy Procedia*, Vol. 78 pp. 388-393.

- Berge, A. & Adl-Zarrabi, B.(2014) Evaluation of vacuum insulation panels used in hybrid insulation district heating pipes. *DHC14, the 14th International Symposium on District Heating and Cooling*, Stockholm, Sweden.
- Berge, A., Adl-Zarrabi, B. & Hagentoft, C. (2013) Determination of specific heat capacity by transient plane source. *Frontiers of Architectural research*, 2(4) 476-482.
- Berge A. (2013) *Novel thermal insulation in future building and district heating applications - hygrothermal measurements and analysis*. Licentiat thesis, Lic 2013:6, Chalmers University of Technology, Göteborg, Sweden.
- Adl-Zarrabi, B. & Berge, A. (2013) *Hybridisolerade Fjärrvärmerör [Hybrid insulation district heating pipes]*, Report 2013:23, Fjärrsyn. (In Swedish)
- Berge, A. & Adl-Zarrabi, B.(2012) Using high performance insulation in district heating pipes. *DHC13, the 13th International Symposium on District Heating and Cooling*, Copenhagen, Denmark.
- Berge, A. & Johansson, P. (2012) *Literature review of high performance thermal insulation.*, Report 2012:2, Chalmers University of Technology, Göteborg, Sweden.
- Adl-Zarrabi, B. & Berge, A. (2012) *Högpresterande Fjärrvärmerör [High perforance district heating pipes]*, Report 2012:16, Fjärrsyn. (In Swedish)
- Berge A. (2011) *Analysis of Methods to Calculate Air Infiltration for Use in Energy Calculations*. Master's Thesis 2011:16, Chalmers University of Technology, Göteborg, Sweden.

## Preface

This thesis summarize my research at the Division of Building Technology, Department of Civil and Environmental Engineering, at Chalmers University of Technology. The research have been funded by the project *homes 4 tomorrow* through *FORMAS*, by the EU project *FC-District* and the three projects *Högpresterande fjärrvärmerör*, *Hybridisolerade fjärrvärmerör* and *Livslängd och statusbedömning av fjärrvärmenät* all funded by *Svensk fjärrvärme* through the research program *Fjärrsyn*.

The field measurements have been made in Varberg, connected to the district heating network of *Varberg Energi*. All prototypes of hybrid insulation district heating pipes have been produced in collaboration with *Powerpipe systems AB*. *Aspen Aerogel* have provided aerogel blankets for the measurements.

I am very grateful to my three supervisors Carl-Eric Hagentoft, Bijan Adl-Zarrabi and Paula Wahlgren. Carl-Eric Hagentoft have been fundamental for the development of my theoretical knowledge through countless discussions. The experimental experience of Bijan Adl-Zarrabi have been invaluable for planning my experiments. Paula Wahlgren and I have had a great pedagogical exchange through our joint teaching. The division of Building Technology have been a great workplace with a good research environment, mainly because of all good colleagues. A special thank to Marek for the company during all hours spent on the road between Göteborg and Varberg.

I also want to thank my family. I thank my parents Karin and Dag for all support and for giving me the foundation on which to build my higher education. Thanks to my brothers Aron, Isak and Leo for all intellectual stimulation which have sharpened my analytical ability.

Most of all I want to thank my wife Bonnie for standing by my side through this whole process.

Axel Berge  
Göteborg, 2016



# Contents

<b>Abstract</b>	<b>iii</b>
<b>List of publications</b>	<b>v</b>
<b>Preface</b>	<b>vii</b>
<b>1 Introduction</b>	<b>1</b>
1.1 Aim . . . . .	2
1.2 Limitations . . . . .	3
1.3 Methods . . . . .	4
1.4 Thesis structure . . . . .	5
<b>2 Nanoporous thermal insulation</b>	<b>6</b>
2.1 Aerogel . . . . .	8
2.2 Vacuum insulation panels . . . . .	10
<b>3 Hybrid insulation district heating pipes</b>	<b>13</b>
3.1 Finite element model for simulations on hybrid insulation district heating twin pipes . . . . .	15
3.2 Thermal performance . . . . .	17
3.3 Optimization of panel configuration . . . . .	19
3.4 Field measurements . . . . .	20
<b>4 Nano-porous insulation in building walls</b>	<b>26</b>
4.1 Wooden stud walls with aerogel blankets . . . . .	27

4.2	Effects from pressure changes in nano-porous insulation . . . . .	29
4.3	Building simulations on building with switchable insulation . . . . .	32
<b>5</b>	<b>Conclusion</b>	<b>35</b>
<b>6</b>	<b>Future work</b>	<b>37</b>
	<b>Bibliography</b>	<b>38</b>

# Chapter 1

## Introduction

The main factors influencing heat transfer through a material between two temperatures is the thickness of the material and its thermal properties: thermal conductivity and specific heat capacity. In nano-porous materials there is a strong relation between the gas pressure and the thermal conductivity.

In a gas, the thermal energy is transferred through collisions between gas molecules. The heat transfer between molecules in a gas is more efficient than the heat transfer from when gas molecules collide with solids. The average distance a gas molecule travels before hitting another gas molecule is called the mean free path. In nano-porous materials, the pore size is of the same magnitude as the mean free path of air, which means a decreasing number of collisions between the molecules in the gas. Therefore the thermal conductivity of the gas is reduced compared to the thermal conductivity of a free moving gas.

The thermal conductivity of a gas in a nano-porous material will also be influenced by the pressure of the gas. A lower pressure means that there are fewer or slower gas molecules which leads to a longer average length between collisions. In other words, a longer mean free path. A consequence of this is that the thermal conductivity of nano-porous materials are sensitive to changes in the pore gas pressure.

The above hypothesis was presented already by Kistler & Caldwell (1934), after Kistler had experienced the low thermal conductivity of his newly invented aerogel (Kistler 1931). The same relation between pressure and thermal conductivity has been found for various aerogels (Fricke et al. 1992, Hümmer et al. 1993) as well as for fumed silica and perlite (Caps & Fricke 2000). Simmler et al. (2005b) show comparative measurements to some materials without nano-pores, where it is clear that a much lower pressure is needed to reduce the thermal conductivity of the gas inside the porous material. The mean free path would reach the same magnitude as the pore size, first at a lower pressure. This relation between pressure and thermal conductivity

has been fundamental for the introduction of vacuum insulation panels (VIP) for the building sector. However, the vacuum in the panels is hard to maintain for long time periods. For nano-porous materials, the vacuum does not need to be of as high quality to achieve a low thermal conductivity, meaning that a larger intrusion of air can be allowed.

For domestic buildings in cold climates, a lower U-value is almost always preferable to save energy. But a lower U-value commonly comes with the cost of an increased wall thickness. Nano-porous insulation could potentially be used to reduce the heat losses without an increase in thickness.

There has been a large number of research projects dealing with VIPs in building components. Some examples of studied applications are flat roof construction with vacuum panels investigated by Brunner & Simmler (2008), wooden stud walls with VIPs between the studs by Haavi et al. (2012) and VIP as a retrofit measure of old buildings with heritage protected façades, as by Johansson et al. (2014). A new area for the VIP research is in applications with a higher temperature around the panels. With a higher temperature, the diffusion of air increases, as shown by Simmler & Brunner (2005a).

A change in pressure could also be utilized to control the thermal conductivity for cases where the optimal properties varies. This is typically true for buildings in cold climates with occasionally large heat loads. Then a low thermal conductivity would be beneficial when heating is needed and a low conductivity would be beneficial when cooling is needed, assuming that the outdoor temperature is below the indoor temperature. A fundamental concept for using vacuum to control the heat losses has been patented by Xenophou (1976) where walls made up of cells can be evacuated by a vacuum pump. Meister et al. (1997) present another concept where the hydrogen pressure can be shifted by electro-chemical reaction with metal hydrides.

This has led to an interest in the research of two applications for nano-porous insulation: Hybrid insulation district heating pipes and as super insulation for buildings which potentially could have switchable properties, controlled by a variation in the internal pressure of the building insulation.

## 1.1 Aim

The aim of this thesis is to evaluate the feasibility of new applications for nano-porous thermal insulation. Two insulation types have been investigated: aerogel blankets and fumed silica vacuum insulation panels. The thesis is parted into two themes correlated to two different applications: hybrid insulation district heating pipes and building insulation, nano-porous insulation in building walls. The thesis tries to answer the following research questions.

On hybrid insulation district heating pipes:

- What effect can nano-porous insulation have on the thermal performance of district heating pipes?
- How can the application nano-porous insulation in district heating pipes be optimized from a heat transfer perspective?
- How will the thermal performance of the hybrid insulation pipes withstand long term usage?

On nano-porous building insulation:

- How will aerogel blankets influence the heat and moisture performance of a wooden stud wall?
- How will a cycling pressure influence the thermal performance of fumed silica and aerogel blankets?
- How can switchable insulation affect the energy performance of a building?

## 1.2 Limitations

All the district heating pipes in this study have been of dimensions between DN 25 and DN 150. Rigid straight pipes have been used and in the twin pipes, the VIPs have been positioned enveloping the supply pipe. For the laboratory measurements, the polyurethane foam (PUR) in the pipes were mixed by hand. This gives a somewhat higher thermal conductivity compared to production line polyurethane foam.

The long term study of the field measurements has been done on pipes connected to a low temperature system. The maximum temperature in the supply pipe was around 90°C. Field measurements at higher system temperatures have been initiated but not analyzed. So far, three years of measurements have been collected.

The properties of aerogel blankets and fumed silica have been tested at various pressures below atmospheric pressure. The measurements have only been performed on material level and not on system level. The measurement results for fumed silica were used for the energy balance simulations of an office. The energy balance have only been made for one office configuration with specific geometry and heat load data.

## 1.3 Methods

The two applications have been investigated from some different angles with a variety of methods. The methods can be divided into three different paths: laboratory measurements, numerical simulations and field measurements.

In the laboratory, a guarded hot pipe apparatus has been used to evaluate the thermal performance of hybrid insulation district heating pipes presented in Paper **I** and Paper **II**. The measurements were based on the standard SS-EN 253 (2009). In this way the results can be compared to commercial pipes, even though the standard measurement is made for homogeneously insulated pipes. In Paper **II**, two apparatuses were used to measure the heat flows in twin pipes. The heat flow was measured for a set temperature difference between the supply and return pipes. A guarded heat flow meter apparatus has been used to measure the thermal conductivity of aerogel blankets in Paper **V** and for both aerogel blankets and fumed silica in Paper **VI**. In Paper **V** the thermal conductivity is measured at various temperatures and at different rates of mechanical compression. In Paper **VI** the samples were enclosed in a plastic bag connected to a vacuum pump, so that the thermal conductivity could be measured at varying pressure. The vapor diffusion coefficient of aerogel blankets was measured by the wet cup method in Paper **V**. The measurements were made for different sample sizes, to find the influence from the edges where the aerogel can crack.

Numerical simulations have been performed using various softwares. The finite element software Comsol multiphysics (2015) was used in Paper **IV** for theoretical estimates of the thermal performance of hybrid insulation district heating pipes. The simulations are used to investigate the potential thermal benefit when introducing VIPs in twin pipe geometries and compares it to the same effect by an increased thickness of polyurethane foam. The thermal bridges in the envelope around the VIP have been modeled in detail to test the influence of variations in configuration. The results from the simulations are also separated between losses from the supply pipe and losses from the return pipe, which is compared to the total losses from the system with and without VIPs. In Paper **V**, Comsol multiphysics (2015) was used to simulate thermal performance at steady-state conditions for different wall assemblies while the finite difference software Wufi2d (2015) was used for transient coupled heat and moisture simulations. The results were analyzed using the model for mold growth potential by Hukka & Viitanen (1999). In Paper **VI**, finite difference method was used in Matlab (2015) to simulate the transient effects on the thermal performance from a pressure change in nano-porous insulation. Finally, Excel was used to calculate the energy performance of a building with switchable insulation in Paper **VII**.

The long term performance of the pipes has been analyzed through field measurements, presented in **III**. Thermocouples have been placed different positions throughout a pipe cross

section, both around the VIP and in corresponding positions in a reference part with only polyurethane foam. The temperatures have been logged over more than three years for the oldest pipe. The resulting temperatures have been analyzed with a superposition model based on Wallentén (1991). The results from the field measurements have been compared to finite element simulations made in Comsol multiphysics (2015). A variation of cases have been simulated, based on either an instant collapse of the VIPs or a slow deterioration from diffusion of gas into the panels.

## 1.4 Thesis structure

In Chapter 2 the theory of nano-porous thermal insulation is presented. The mechanisms for heat transfer in porous and nano-porous materials are described, followed by a description of aerogel and vacuum insulation panels. Next, Chapter 3 will present the first theme of the thesis: *hybrid insulation district heating pipes* and will be followed by the research results from Paper **I-IV**. Chapter 4 will present the second theme: *nano-porous building insulation* from Paper **V-VII**. The thesis will finish with a summary of the conclusions in Chapter 5 and suggestions for future work in Chapter 6.

# Chapter 2

## Nanoporous thermal insulation

In thermal insulation, porous materials are commonly used. The porous structure utilize the low thermal conductivity of the gas in the pores. At the same time, heat radiation and gas convection is hindered by the solid structure. The effective thermal conductivity of porous material can in a simplified way be described as in Equation (2.1), assuming that the heat transfer through convection can be neglected:

$$\lambda_{insulation} = \lambda_{solid} + \lambda_{gas} + \lambda_{radiation} \quad [W/(m \cdot K)] \quad (2.1)$$

where  $\lambda_{insulation}$  is the apparent thermal conductivity of the insulation material ,  $\lambda_{solid}$  is the thermal conduction through the solid structure of the pore walls,  $\lambda_{gas}$  is the conduction through the pore gas and  $\lambda_{radiation}$  is the heat radiation between the cell walls. The thermal conductivity will also be affected by some coupling effects as shown by Ebert (2011).

The benefit of nano-porous materials is that the small pores hinder the heat transfer through the gas in the pores, reducing the term  $\lambda_{gas}$  in Equation (2.1). The reason for the decrease is that collisions between the gas molecules and the solid pore walls transfer less heat than the collisions between gas molecules. With smaller pores the probability of colliding gas molecules is reduced in favor of collisions against walls (Baetens et al. 2010a). The average distance a gas molecule travels before colliding with another gas is called the mean free path,  $l_{avg}$ , and can be calculated by Equation (2.2):

$$l_{avg} = \frac{k_B T}{\sqrt{2} \pi d^2 P_g} \quad [m] \quad (2.2)$$

where  $k_B$  is the Boltzmann constant [ $\text{Pa} \cdot \text{m}^3/\text{K}$ ],  $T$  is the temperature [K],  $d$  is the molecule diameter [m] and  $P_g$  is the gas pressure [Pa]. The mean free path of air is around 100 nm at

normal pressure and temperature. This means that for air filled porous materials with a pore size some magnitudes above 100 nm, most gas molecules will collide with other gas molecules and the solid structures influence on the thermal conductivity can be neglected. For pore sizes in the range of the mean free path and below, the solid walls would interrupt the heat transfer. The conductivity of the gas can then be calculated according to Equation (2.3) (Ebert 2011),

$$\lambda_g = \frac{\Pi \cdot \lambda_{g,0}}{1 + 2\beta(l_{avg}/\delta)} \quad [W/(m \cdot K)] \quad (2.3)$$

where  $\lambda_g$  is the gas conductivity in limited spaces [W/(m·K)],  $\Pi$  is the porosity of the material [-],  $\lambda_{g,0}$  is the gas conductivity for a free gas [W/(m·K)],  $\beta$  is a constant correlated to the magnitude of the energy exchange between the gas and the solid walls [-] which has a value between 1.5 and 2 (Baetens et al. 2010a) and  $\delta$  is the characteristic system size [m]. The relation between the mean free path and the characteristic system size,  $l_{avg}/\delta$ , is commonly referred to as the Knudsen number,  $Kn$  [-]. With the mean free path of air and a porosity close to 1, Equation (2.3) gives the relation  $\lambda_g/\lambda_{g,0}$  as in Figure 2.1.

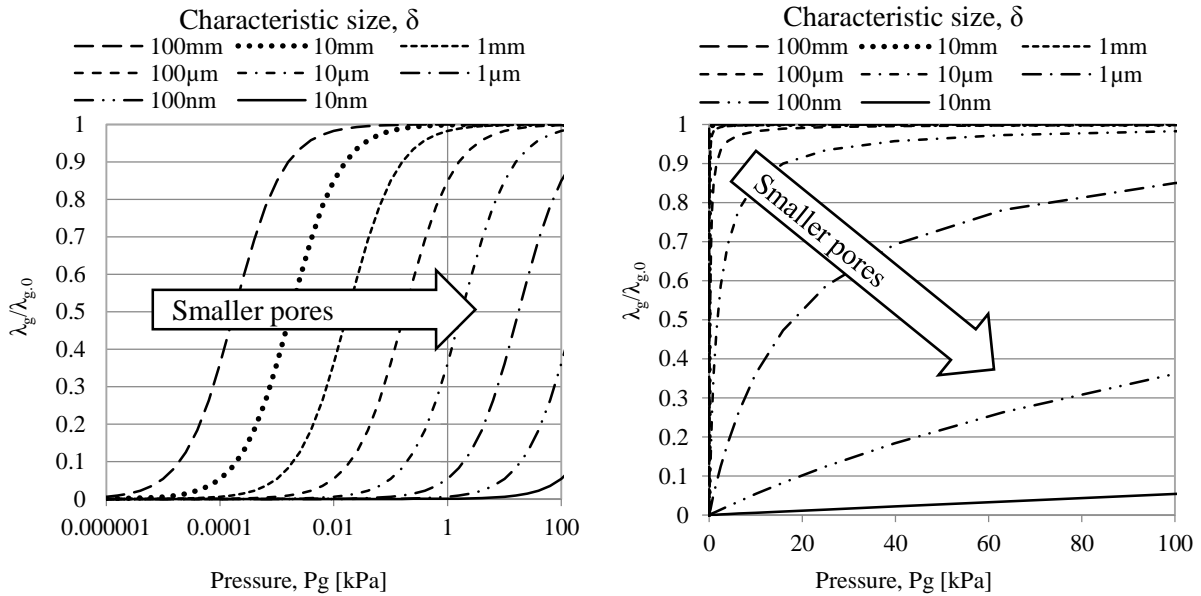


Figure 2.1: Principal figure of thermal conductivity through the air in a porous insulation for different pressures below atmospheric pressure (just above 100 kPa). To the left, the pressure axis is logarithmic and to the right the pressure axis is linear. The porosity of the material is assumed to be 1.

As seen in Equation (2.2), the mean free path is inversely proportional to the gas pressure. In Equation (2.3) the denominator includes one plus the quotient between mean free path and pore size. This means that when the mean free path is small compared to the pore size, the denominator will be one. At lower pressures the mean free path will increase and thereby, the thermal conductivity will decrease. As seen in Figure 2.1, a large pressure change is needed

if the pores are large, but, if the pores are small the relation between pressure and thermal conductivity becomes almost linear.

## 2.1 Aerogel

Aerogels are former gels which have been dried under such circumstances that the solid structure of the gel is preserved. Kistler (1931) had the hypothesis that the main reason for the shrinkage when a gel is dried to a xerogel were the forces from the pore liquid pulling the pore walls together. He tested the hypothesis by drying gels in a condition of temperature and pressure above the critical point. At that state, the fluid in the pores could be exchanged with a gas without any forces on the structure. With the right gel, this led to a material with very high porosity and a pore size in the nano range.

Already Kistler & Caldwell (1934) realized the superb thermal performance of the aerogels. And he assumed that the reason for the low thermal conductivity was the small pores in accordance with Equation (2.3). The properties have later been investigated by several methods and researchers (Baetens et al. 2010a). A monolithic piece of silica aerogel is shown in Figure 2.2.



Figure 2.2: Monolithic silica aerogel. (Photo: Nina Zanders)

Since aerogels can be transparent they are interesting for light inlet into building. Scheuerpflug et al. (1985) investigated the thermal performance of transparent aerogels. They present how the radiative properties influence the total heat loss through the aerogel. The performance of the aerogel could be improved further by hindering the radiation through the material, at the cost of losing the transparency. Nilsson et al. (1986) used the hot strip method to measure the thermal conductivity of a transparent aerogel and found it to be  $17 \text{ mW/m}\cdot\text{K}$ . Reim et al. (2004) measures the thermal conductivity and the optical properties of two types of aerogel granulates. They tested the influence of mechanical loading of the aerogels. The loading improves the thermal performance, and some of the improvement sustains after the load was removed. The load compact the granulates and since the thermal conductivity of the aerogel is lower than the thermal conductivity of the air the apparent thermal conductivity decreases.

Fricke et al. (1992) investigated the addition of opacifiers, soot or titanium oxide, to optimize the thermal conductivity of monolithic aerogels. They find a minimum thermal conductivity of 13 mW/m·K at a density of 12 kg/m<sup>3</sup>. Hümmer et al. (1993) measured the thermal conductivity of aerogel granulates and powders with a guarded hot plate apparatus. The granulates and powders are shown to have a thermal conductivity 17-22 mW/m·K. Compared to the monolithic aerogel measured by Fricke et al. (1992), a lower pressure is needed to decrease the thermal conductivity. However, the minimum thermal conductivity at very low pressures are shown to be lower for some of the powder samples. Spagnol et al. (2009) measured monolithic and granular aerogels with the guarded thin film method with similar results. The change in thermal conductivity was also shown to decrease in a stepwise manner rather than as one large step as for the ideal case in Figure 2.1. This is probably a consequence of two superpositioned pore systems, one within the granulates and one between the granulates for which the effect of the pressure decrease follows different curves. Pietruszka et al. (2012) made measurements on an aerogel blanket composite with a thermal conductivity of 15-16 mW/m·K. With reinforcement fibers the strength of the aerogel is considerably improved.

The reason for the low thermal conductivity of aerogels are their small pores. Tamon et al. (1997) measured the pore size distribution of a 200 kg/m<sup>3</sup> aerogel with a N<sub>2</sub> adsorption method. The pores were shown to be in the range of 1-100 nm with the main volume around 10 nm. The optimal density for thermal conductivity was found around 100 kg/m<sup>3</sup> by Fricke et al. (1992), but the density could be much lower. Tillotson & Hrubesh (1992) produce an aerogel with a density of 3 kg.

Aerogels can also be made hydrophobic, as shown for an aerogel blanket sample in Figure 2.3. Even though their aerogel blankets were hydrophobic, Pietruszka et al. (2012) showed that the blankets could be water filled through immersion and later be sensitive to freeze thaw cycling.

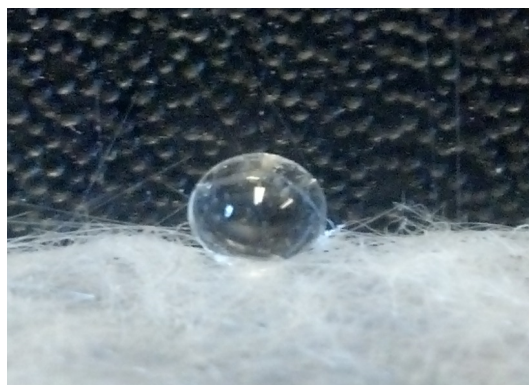


Figure 2.3: Water droplet on a hydrophobic aerogel blanket.  
(Photo: Axel Berge)

The research on the application of aerogels has been limited. Pietruszka & Gerylo (2010) investigate the use of aerogel blankets in curtain wall frames. With the use of material data for

aerogel blankets, the U-value of the frame was found to be  $0.83 \text{ W/m}^2\text{K}$ . A value comparable to passive house standard windows.

Some research has been made on using the transparent properties of aerogel to collect solar energy. Schreiber et al. (1986) investigate the use of transparent aerogel to let sun through to a stone wall and then keeping the heat from the solar radiation in the wall. Svendsen (1992) use transparent aerogel to insulate solar collectors.

Rubin & Lampert (1983) investigate the solar transmittance on an aerogel with a thermal conductivity of  $19 \text{ mW/m}\cdot\text{K}$ . The total transmittance of a 8 mm aerogel between two normal window glasses was found to be 0.6 which is similar to the transmittance of a 3 pane window. Reim et al. (2005) investigate the use of noble gas filled aerogel granulates in translucent daylight inlets. With a light transmittance of 0.24-0.54 the U-value is  $0.44\text{-}0.56 \text{ W/m}^2\text{K}$ .

## 2.2 Vacuum insulation panels

Vacuum insulation panels (VIP) consist of a porous core material that has been evacuated and put in a highly diffusion tight envelope. An opened VIP with a fumed silica core is shown in Figure 2.4. To minimize the permeation of gas into the vacuum panel the envelope commonly contain some layers of aluminum, which have a high thermal conductivity, many orders of magnitude higher than the evacuated core of the VIP. This creates an optimization problem where an increased aluminum thickness decrease the permeation and prolongs the life span of the panel, but at the same time, it creates thermal bridges along the edges of the panel. Three main characteristics are thereby of importance for the thermal performance of a VIP: the thermal performance of the core material, the thermal bridge effect through the envelope and the permeation of gas into the panel.

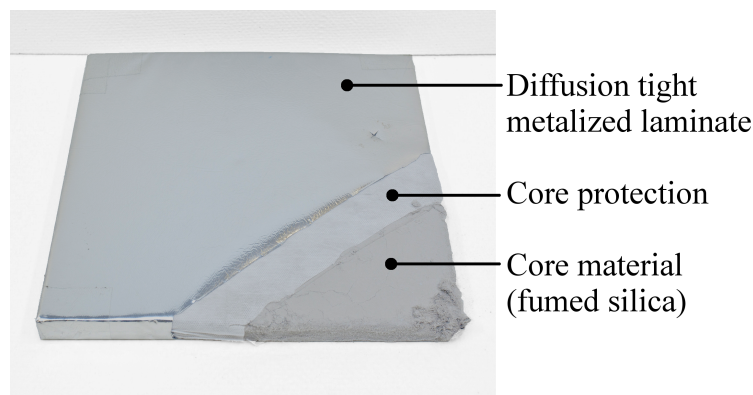


Figure 2.4: The layers of a vacuum panel with a fumed silica core.  
(Photo: Nina Zanders)

The core material in a VIP has to meet two criteria: the pore system must be open so that the air can be evacuated and it must be strong enough to withstand the pressure of the atmosphere. For building application the expected life span of the VIP is long. Therefore a nanoporous material is preferable since it will retain its good thermal performance even at higher pressures. This can be seen in Simmler et al. (2005b) where glass fiber insulation is shown to give lower thermal conductivity at the minimum pressure but the fumed and precipitated silica materials decrease in thermal conductivity at not o low pressures. Glass fiber has therefore been used for applications with shorter expected life time. Caps & Fricke (2000) test different nanoporous filler materials for use in vacuum insulation panels: fumed silica, percipitated silica, aerogel powder and perlite. Precipitated silica is most promising with a thermal conductivity below 5 mW/m·K at pressures up to 1-2 kPa.

There are two types of envelopes commonly used in VIPs for the building sector. Aluminum foils and metalized films. In aluminum foil envelopes, the foil is glued in between two polymer films. The foil commonly has an aluminum thickness around 10  $\mu\text{m}$ . In a metalized film, the aluminum is instead deposited directly onto the surface of a polymer film. This enables a much thinner aluminum layer down to thicknesses of 20 nm. Although, the thinner layers are more sensitive to pointwise defects. In most VIP envelopes multiple layers are compiled in a laminate.

The thermal conductivity of aluminum is about 200 W/m·K, 5 orders of magnitude larger than the thermal conductivity of an evacuated VIP core. Ghazi Wakili et al. (2004) have made measurements with guarded hot plate on three types of VIP, with and without an envelope edge in the measurement area. Two samples had metalized films and showed a 10-20% increase in effective thermal conductivity due to thermal bridges in a 1 m<sup>2</sup> panel. The last VIP had a foil envelope and the effective thermal conductivity almost doubled compared to the center of panel thermal conductivity. Ghazi Wakili et al. (2011) continue the guarded hot plate measurements on multilayer VIP structures. With multiple layers the influence of the thermal bridges can be reduced. The measurements are compared to simulations with good correlation. In the simulations, the envelope was treated as a single representative layer. Sprengard & Holm (2014) simulates the difference between single layer edges of the panels and double, layered edges where the double layers represent the seams of the envelope. The distance between panels and fasteners are also investigated. The double layer edges is shown to almost double the heat loss. Tenpierik & Cauberg (2007) developed an analytical model to evaluate the thermal bridges at the VIP edges. The model shows less than 5% error when compared to numerical simulations. One of the main simplifications of the model was that the thermal conductivity of the core was assumed to be 0 mW/m·K. This meant that for panels with a high thermal conductivity the deviation between simulations and measurements increase.

The thermal bridge effect of the vacuum insulation is in a direct relation to the long term

performance. With a thinner envelope the long term performance is reduced. Simmler & Brunner (2005a) evaluated the long term performance of VIPs for building applications. For a VIP with a production thermal conductivity in the center of the panel of  $4 \text{ mW/m}\cdot\text{K}$  they suggest a 25 year design value of  $6 \text{ mW/m}\cdot\text{K}$  if an aluminum foil is used or  $8 \text{ mW/m}\cdot\text{K}$  if a metalized film laminate is used. Schwab et al. (2005) measured the permeation through different VIP envelopes. The internal pressure was measured through the foil Lift-off Procedure where the sample is put in a vacuum chamber and the pressure was changed until the envelop lifts from the surface of the core material. They indicate that the area of the panel is more important for water vapor permeation, but for air transmission the sealing has a larger effect. For the two better performing films, the air transmission at  $80^\circ\text{C}$  was around 5 times the rate at  $25^\circ\text{C}$ . Araki et al. (2009) tested different polymers for the vacuum panel envelope and show that there are plastics that can withstand a higher temperature than the polyethylene used in most films today. Although, with a higher melting temperature, a higher temperature is needed to seal the VIP envelopes.

# Chapter 3

## Hybrid insulation district heating pipes

Statistics Sweden (2013) collects yearly statistics on Swedish energy usage. They show that approximately 10% of the energy produced for district heating is lost from the distribution system. According to Reidhav & Werner (2008) this number could be even higher for areas with a sparse energy outtake. For the 72 sparse areas under investigation the worst had distribution losses above 40%.

International Energy Agency's District Heating and Cooling Annex VIII (IEA DHC Annex VIII) (Zinko et al. 2008) presents some suggestions to reduce the heat losses from district heating pipes:

- To use twin pipes instead of two single pipes, where the supply pipe and the return pipe are placed within the same insulation pipe.
- To shift the symmetry of the twin pipe so that the warmer supply pipe gets more insulated:
  - by different sizes on the supply and return pipe.
  - by shifting the position of the supply and return pipes so that the supply pipe is closer to the center.
  - by using an egg shaped casing with thicker insulation around the supply pipe.
- To put more than two pipes within the same insulation where some can be turned off when the energy outtake is low.
- To add some superior type of insulation close to the supply pipe.

The use of twin pipes is already common practice in Sweden, when applicable. The shift of the supply pipe towards the center of the surrounding pipe has been investigated by Dalla Rosa et al. (2011) who show a reduction by up to 3.2%. Bøhm & Kristjansson (2005) investigate egg

shaped casing pipes and show a reduction of 7% compared to twin pipes. Bøhm & Kristjansson (2005) also investigate the use of two supply pipes with one pipe turned off when the outtake is low. This led to a decrease in the energy loss of around 25% compared to twin pipes. The last suggestion from IEA-DHC (Zinko et al. 2008), to add a superior type of insulation around the supply pipe, has been tested in this study.

In a cylindrical geometry, the insulation close to the center has a larger influence on the total heat loss. This can be explained by the equation for thermal conductance,  $K$ , through a cylindrical layer in Equation (3.1) (Hagentoft 2005):

$$K = \frac{2\pi L\lambda}{\ln(\Delta r/r_1 + 1)} \quad [W/K] \quad (3.1)$$

where  $L$  is the pipe length [m],  $\lambda$  is the thermal conductivity of the layer [W/(m·K)],  $\Delta r$  is the layer thickness [m] and  $r_1$  is the inner radius of the cylindrical layer [m]. If the inner radius,  $r_1$ , increases, then the denominator decreases and the total conductance increases. The insulation closer to the center is thereby more material efficient. This indicates that it might be preferable to add a more expensive high performance insulation close to the center of the pipe, rather than add insulation thickness to the outside of the pipe. This has led to the development of a concept for hybrid insulation district heating pipes, presented in Figure 3.1. The innermost part of the polyurethane foam (PUR) in a conventional district heating pipe is exchanged with a high performance insulation. For a twin pipe, the high performing insulation surrounds the supply pipe.

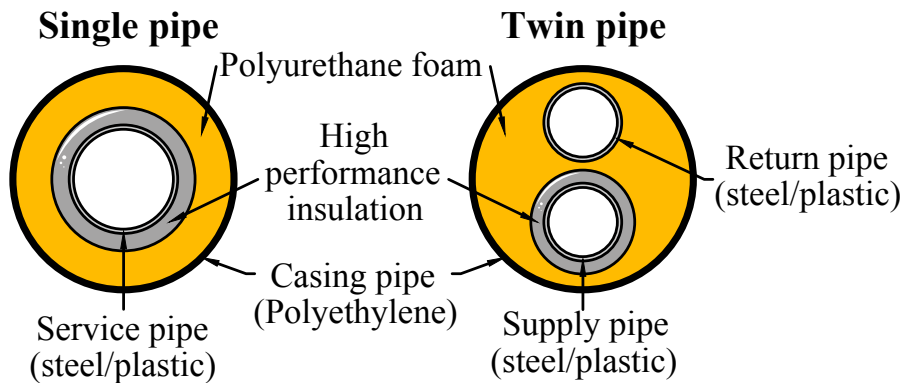


Figure 3.1: Concept for hybrid insulation district heating pipes.

Early in the research, VIPs were chosen as insulation, motivated in Section 3.2 and in Paper I. One important aspect for the thermal performance of VIPs is the thermal bridges created in the highly diffusion tight envelope. The envelop must surround the whole panel to hinder gas from entering and destroying the vacuum. The thermal bridges in a pipe are described in Figure 3.2. There is a thermal bridge along the panel where it overlaps itself (TBA), a thermal bridge at the edges of the panel (TBE) and in twin pipes there is a reallocation of heat from the warm

spot in between the pipes out into the insulation (TBT).

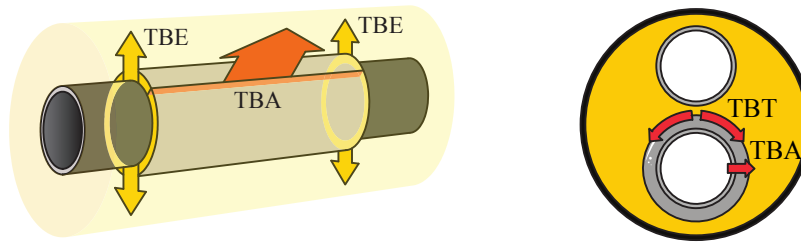


Figure 3.2: Description of the thermal bridges in the vacuum panel. The left image describes the thermal bridges at the edge of the panel (TBE) and along the panel (TBA). The right image shows a cross section of a twin pipe which also has a thermal bridge between the service pipes (TBT).

### 3.1 Finite element model for simulations on hybrid insulation district heating twin pipes

A twin pipe in the ground can be modeled analytically with the multipole method as shown by Wallentén (1991), although, the multipole method can only handle circular boundaries. For hybrid insulation pipes with VIPs, the thermal bridge in the envelope will cross the circles and is thereby not covered by the model. Finite difference is commonly used for heat simulations in buildings, and has been used to model VIPs by for example Ghazi Wakili et al. (2004), and Sprengard & Holm (2014). To use finite difference in a cylindrical geometry, some geometrical transformation is needed. This has led to the choice of using the finite element method instead, through the software Comsol multiphysics (2015), similar to the simulations by Dalla Rosa et al. (2011) and Bøhm & Kristjansson (2005). A triangular mesh can give a good approximation of a cylindrical geometry.

For most simulations a two dimensional model was used. Depending on the analysis, the ground was modeled either as a square domain with adiabatic edges at all sides but upwards, or as a cylindrical domain surrounded by a ground surface boundary, as presented in Figure 3.3. The implication of using the different models is discussed in Paper IV. In early simulations it was seen that the temperature dependence of the thermal conductivities had a large impact on the results. Especially since the introduction of the vacuum panel decreases the temperature of the PUR, improving its thermal conductivity.

The main complication of the model is the thermal bridge through the envelope. A substantial amount of modeling has been made for the heat flow through the edges of flat VIPs, using some different assumptions and model simplifications. Ghazi Wakili et al. (2004) compile

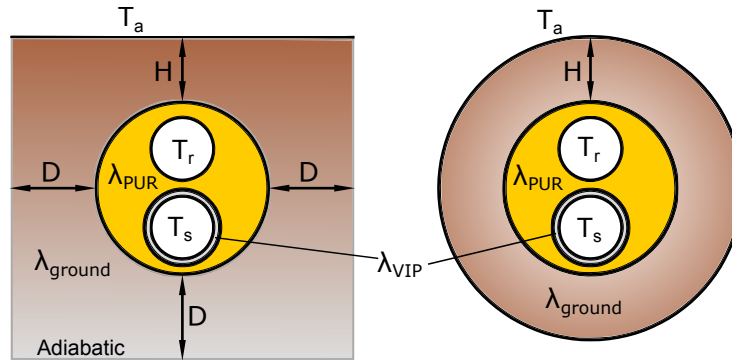


Figure 3.3: Description of the two dimensional simulation models with a square domain to the left and with a circular domain to the right.

each layer in the envelope laminate with the same material into one layer with the combined thickness of all layers. A similar approach was used by Sprengard & Holm (2014). Willems et al. (2005) instead combine all film materials into a combined material layer with the total thickness of all layers and a representative thermal conductivity. Since finite elements calculate the temperatures at the edges of the elements, the thin envelope can instead be modeled as a layer without a geometric thickness. This assumes that the thermal resistance perpendicular to the film can be neglected, compared to the thermal resistance in the surrounding insulation. Thereby, the temperature on each side of the film is the same. Paper IV shows that this is a reasonable assumption for the film layer. Another simplification made in the model in Paper IV is to neglect the influence of air cavities and sealing folds. Since the conclusions drawn from the simulations investigate the consequence of variation rather than the exact heat losses, the simplifications are assumed to be reasonable. The overlap of the VIPs around the pipe has thus been modeled according to Figure 3.4

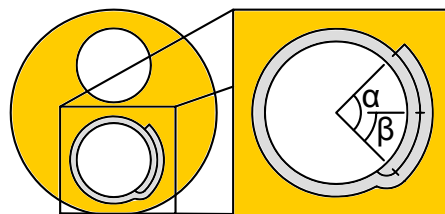


Figure 3.4: Definition of the VIP overlap. The overlap is defined by two angles,  $\alpha$  and  $\beta$ . The angle  $\alpha$  correspond to the overlap length and the angle  $\beta$  correspond to the placement of the beginning of the overlap, relative to the horizontal axis.

## 3.2 Thermal performance

Heat loss measurements are presented in Paper **I** for single pipes and in Paper **II** for twin pipes. The heat losses have been measured with a guarded hot pipe apparatus based on the standard measurement from SS-EN 253 (2009). The outcome of the standard measurement is the thermal conductivity of the insulation material. In a hybrid insulation pipe, two materials are used. So, the measured thermal conductivity is a representative value for the total thermal resistance of the hybrid insulation. Thereby, the results are only representing the geometry of the measured sample.

Paper **I** presents measurements on single pipes with aerogel blankets and fumed silica VIPs. The production of the VIP pipe is shown in Figure 3.5. The results have been presented as representative thermal conductivities, both for the whole pipe and for the superinsulation layer. The measurement results are shown in Table 3.1. For these single pipes the heat losses are reduced by up to 29% for the 10 mm thick VIP. The vacuum panels have a considerably higher calculated thermal conductivity than properties presented by Simmler et al. (2005b). This is assumed to mainly be a consequence of the thermal bridges in the envelope of the VIP. There is also a slight variation of the thickness of the VIP when it is bent to a cylinder which would create some deviation from theoretical calculations. Finally, the high temperature close to the pipe will increase the thermal conductivity of the VIP. The thermal conductivity is still around 60% less than for PUR. The VIPs and the aerogel blankets have a similar cost, while the VIPs have a considerably larger effect on the thermal conductivity. This led to the choice to continue the research with the VIPs.



Figure 3.5: Prototype production of hybrid insulation district heating pipe with vacuum insulation panels.

In Sweden, twin pipes are common to use for smaller dimensions of pipes. Therefore, measurements were also done for twin pipes with a VIP around the supply pipe, presented in Paper **II**.

Table 3.1: Apparent thermal conductivity of the prototype single pipes. The reduction is in comparison to the reference pipes.

Size		Thermal conductivity [mW/(m·K)]	Reduction [%]
<b>Polyurethane foam references</b>			
Reference	DN 80/180	27.8	-
Reference	DN 100/225	27.8	-
Production quality PUR	-	26	-
<b>Whole pipes</b> (compared to reference pipes)			
Vacuum insulation panel, 5mm	DN 100/225	23.5	15
Vacuum insulation panel, 10 mm	DN 100/225	19.6	29
Aerogel blanket, 10 mm	DN 80/180	24.0	14
<b>Superinsulation layer</b> (compared to production quality PUR)			
Vacuum insulation panel, 5 mm	-	11.2	57
Vacuum insulation panel, 10 mm	-	10.3	61
Aerogel blanket	-	17.9	31

The twin pipes had the dimensions DN 2\*80/315 with various thickness and overlap length of the VIPs. The heat flows from the pipes were measured at temperature levels proportional to those used in the simulations in Paper **IV**, which is based on typical grid temperatures. This way, the relative performance can be compared. The results are shown in Table 3.2. The total energy losses from the twin pipes are reduced by around 15% when hybrid pipes are compared to conventional pipes with the same dimensions. But, the losses from the supply pipe was reduced by up to 39%. This can be compared to the results from the simulations in Paper **IV**, presented in Table 3.3. In the simulations, the VIP thickness is only 8 mm and 2 different thermal conductivities have been used for the VIP envelope:  $\lambda_{05}$  and  $\lambda_{20}$  at 0.5 W/m·K and 20 W/m·K respectively. The overlap in the simulations were 45° of the circumference, close to 35 mm.

Table 3.2: Heat losses from twin pipes measured with two heating rods, one in each service pipe. The temperatures were 80°C in the supply pipe, 58°C in the return pipe and 22.5°C in the laboratory.

	Heat flow [W]			Reduction [%]		
	Supply	Return	Total	Supply	Return	Total
Reference	9.6	2.2	11.8	0	0	0
10 mm VIP, 0 mm overlap	6.8	3.5	10.4	29	-61	12
10 mm VIP, 60 mm overlap	6.1	3.8	10.0	36	-74	16
10 mm VIP, 100 mm overlap	6.0	3.8	9.7	38	-70	18
15 mm VIP, 60 mm overlap	5.8	3.9	9.7	39	-78	17

Table 3.3: Simulated heat losses from district heating pipes in the ground with 8 mm VIPs. The identifiers  $\lambda_{05}$  and  $\lambda_{20}$  correspond to the envelope thermal conductivity, at 0.5 W/m·K and 20 W/m·K respectively

Size		Heat flow [W]			Reduction [%]		
		Supply	Return	Total	Supply	Return	Total
Reference	DN 2*80/250	17.0	6.0	23.1	0	0	0
$\lambda_{05}$	"	8.0	7.8	15.8	53	-29	31
$\lambda_{20}$	"	9.1	7.7	16.8	47	-28	27
Reference	DN 2*80/315	11.5	2.7	14.2	0	0	0
$\lambda_{05}$	"	6.4	4.3	10.8	44	-61	24
$\lambda_{20}$	"	7.2	4.1	11.3	37	-52	20

### 3.3 Optimization of panel configuration

In hybrid insulation district heating twin pipes, there is no symmetry because of the thermal bridges at the panel edge. As a consequence, the rotation of the panels matters. For the simulations of the thermal bridges, two envelope compositions have been investigated: one with a thermal conductivity of 0.5 W/(m·K) and one with a thermal conductivity of 20 W/(m·K), referenced to as  $\lambda_{05}$  and  $\lambda_{20}$  respectively. The influence of the rotation was investigated through simulations with Comsol multiphysics (2015) in Paper **IV**.

To evaluate the rotational position, a configuration with a 45° overlap angle  $\alpha$  was used. The positioning angle  $\beta$  from Figure 3.4 was varied. The results are shown in Figure 3.6 for  $\lambda_{05}$  to the left and for  $\lambda_{20}$  to the right. Depending on the thermal conductivity of the film, the curves show opposite behavior. With a low thermal conductivity of the film, the extra thickness of the insulation in the overlap will dominate and the optimal place for the overlap is where the temperature gradients are the largest. This happens for a  $\beta$  around 110° when the overlap is pointing downwards. With the higher thermal conductivity, the heat flow through the thermal bridge dominates and the optimum position is contrary the position with the smallest thermal gradients, between the supply and return pipe.

Similar results are shown when the influence of the overlap length is tested. Two cases for the positioning of the panels were compared, either  $\beta = 0^\circ$  or  $\beta = \alpha$  corresponding to a fix position of the inner edge of the overlap or a fixed position of the outer edge. The results are shown for the two thermal conductivity levels in Figure 3.7. The results show that an addition of high performing insulation could actually increase the heat losses if the position of the thermal bridge is not considered. The results also indicate that the outer edge of the thermal bridge has the main influence on the optimum placement of the thermal bridge for a high conductivity envelope. When the outer edge is rotated,  $\beta = 0$ , the results fluctuate while a fixed outer edge,  $\beta = \alpha$ , the reduction in heat loss is almost linear with the addition of insulation.

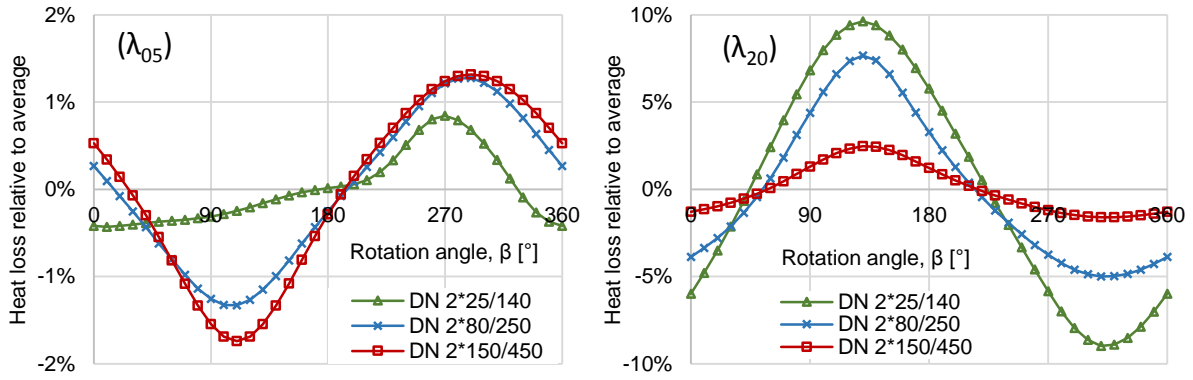


Figure 3.6: The heat loss relative to the average for a variation in the rotational position,  $\beta$  of the VIPs.

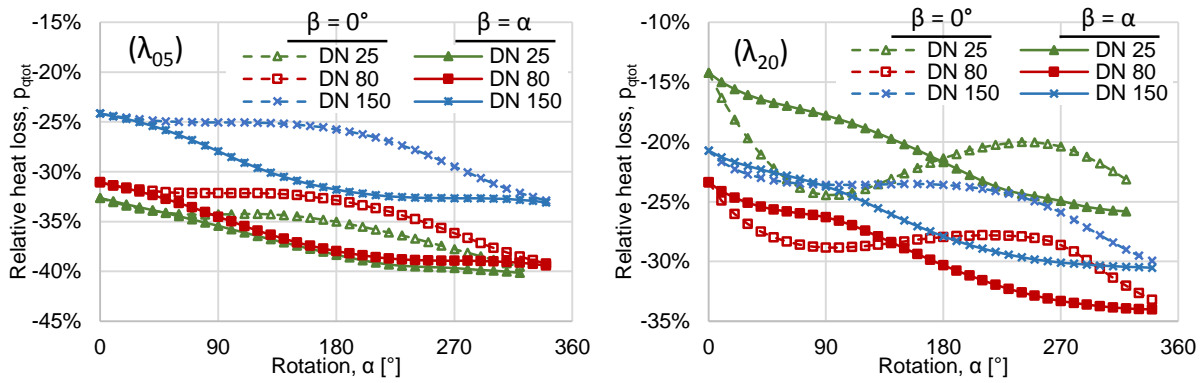


Figure 3.7: The heat loss relative to a reference PUR pipe depending on the length of the overlap.

### 3.4 Field measurements

Bøhm (2001) compares different methods to evaluate the heat losses from district heating pipes in field. The ground surface temperature methods would be problematic for the hybrid pipe measurements since we only have short distances of pipes. The rest of the pipe with conventional insulation would influence the results. A heat flow meter could give good results of the total losses but Bøhm (2001) points out some problems with calibration. Another problem with heat flow measurements on the casing is that you cannot separate the losses from the supply pipes and the return pipes. Therefore, thermocouples were used to measure the temperatures at different positions through the pipe section. These measurements can later be fit to simulation results in order to obtain the heat flows. The thermocouple measurements could also give point-wise information on thermal performance which could be used to investigate the influence of thermal bridges in the vacuum panel.

Two 6 m long sample pipes, of which half was insulated with VIPs and the other half was used as reference, have been connected to the district heating network in Varberg on the Swedish west coast. The network is a low temperature network with the maximum registered temperatures

below 90°C. The position for the temperature measurements are shown in Figure 3.8, where S and R represent the supply and return pipes, u, s and d represent the up, side and down position around the pipe and VIP and PUR represent the hybrid insulation part (with VIPs) and the reference part (with only PUR). In addition, the temperature in the measurement station has been measured and is referred to as  $T_a$ . The temperatures have been measured on the outside of the vacuum panel and at the same position in the middle of PUR for reference. From the measured points and outwards, the pipes are identical. With a lower measured temperature, there is a lower temperature gradient between the measurement point and the ground, and thereby a lower heat loss.

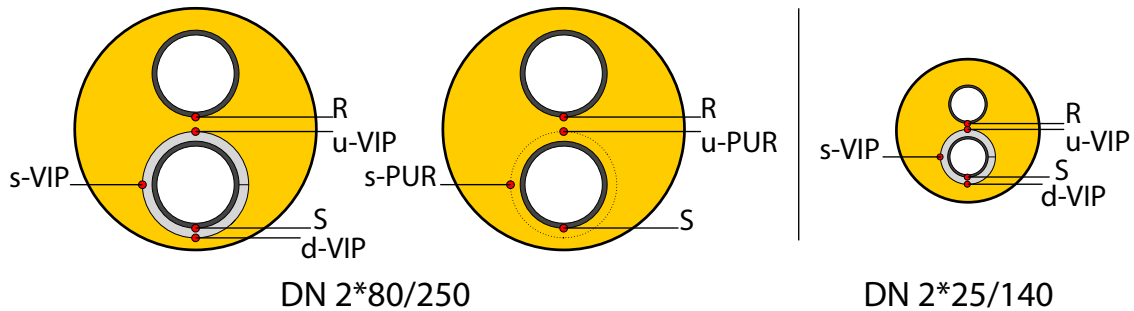


Figure 3.8: Position of thermocouples in the field measurement pipes. Each point is measured in at least two positions along the pipe.

The thermal performance is indicated by the temperature difference between the temperature on the VIP and the corresponding reference temperature. The resulting temperature measurements for one of the pipes are shown in Figure 3.9. The results are presented as a boxplot showing the minimum/1st quartile/median/3rd quartile/maximum of the measured temperature. The thermocouple for position R-1 was damaged and thereby the box is filled. Otherwise, the results show a considerably lower temperature on the backside of the VIPs compared to the same position in the PUR. This means that the heat losses are less than for a conventional PUR pipe. However, the magnitude of the difference in heat flow is complex to evaluate.

The temperatures in Figure 3.9 show good consistency between measurements at the same position along the pipe. The measurements in PUR have larger variations, probably due to the challenge of positioning the thermocouples at an exact position.

The thermal performance of VIPs depends on the ability of the VIP to separate the vacuum from the surrounding. Simmler & Brunner (2005a) have tested the long term performance of VIPs. They show that the pressure increasing rate increase considerably with temperature. This correlates well with the effect predicted by the Arrhenius equation where the diffusion is exponentially dependent on the temperature. The VIP can be parted into two diffusion paths: through the surface of the envelope and through the seals of the envelope.

In a district heating pipe, the temperature will be high compared to the temperature load

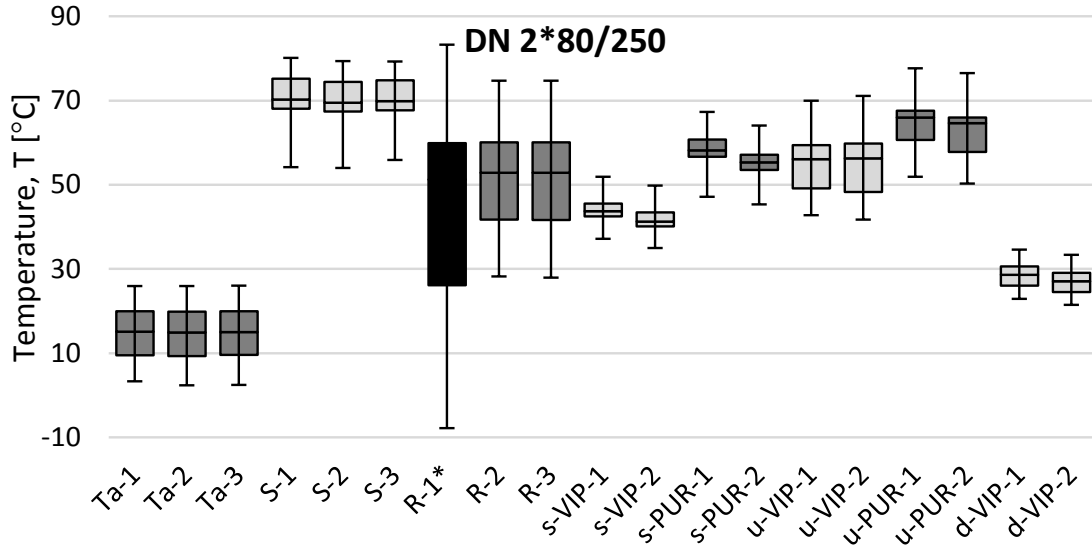


Figure 3.9: Boxplot of the temperature measurements in the pipe with dimensions DN 2\*80/250. The boxes show the minimum/1st quartile /median /3rd quartile/maximum of the measured temperatures. The temperatures are presented in alternating dark and light color corresponding to the same measurement position.

on building insulation, even though the life time expectancy is in the same magnitude. This indicates that VIPs for district heating need a higher performing envelop. Also, the the polymers in the film typically have a melting point around 100°C and a somewhat lower temperature where it is destroyed (Araki et al. 2009).

The temperature measurements in Paper **III** have been used to estimate the long term performance in the VIPs. A model for the temperatures were developed, based on the assumption that the temperature in any point can be calculated from the superposition of a symmetrical and an asymmetrical case, presented in Figure 3.10, by Equation (3.2).

$$T(x, y) = T_{\sigma} \cdot A(x, y) + T_{\alpha} \cdot B(x, y) + T_a \quad [^{\circ}C] \quad (3.2)$$

where  $T_{\sigma}$ ,  $T_{\alpha}$  and  $T_a$  are the symmetrical, asymmetrical and ambient temperature as defined in Figure 3.10. The constants  $A$  and  $B$  are related to the point where the temperature is investigated.

The model is based on some fundamental assumptions.

- The properties are independent of time, or age. This is the main assumption and the problem we are investigating. Based on the idea that we can compare the model, which is stable in time, to our field measurements.

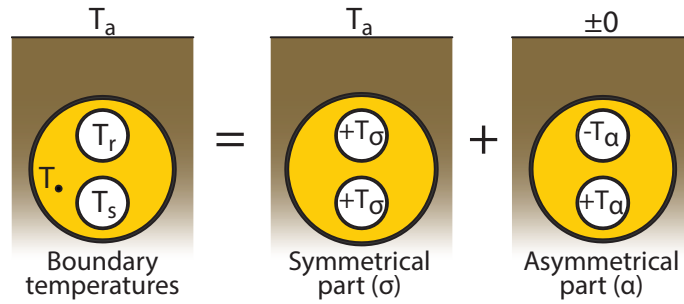


Figure 3.10: Description of the temperatures in the superposition model.

- The temperature dependency of the thermal conductivities can be neglected. This effect will create an error but it will balance itself with the variation in temperatures.
- The influence of thermal mass can be neglected. Which is a reasonable assumption when using average values over full seasonal cycles for the boundary temperatures.

The constants  $A$  and  $B$  can be calculated with the least square method from the measurements. When the constants are used with the measured boundary data, the difference between the calculated and the measured temperature shows the error in the model, as calculated by Equation (3.3):

$$T_{dev} = T_{supos} - T_{meas} \quad (3.3)$$

where  $T_{dev}$  is the deviation ( $^{\circ}\text{C}$ ),  $T_{supos}$  is the calculated temperature according to the superposition model ( $^{\circ}\text{C}$ ) and  $T_{meas}$  is the measured temperature in the assessed point ( $^{\circ}\text{C}$ ).

If the model overestimates the temperature early and underestimates the temperature later on, then it is an indication of a deterioration of the thermal conductivity.

To evaluate the size of the deterioration, transient simulations were made with Comsol multiphysics (2015), similar to the model described in Section 3.1. Five different cases were simulated, with different changes in thermal conductivity over time, as presented in Figure 3.11. Case 0 is a reference case with no variation in the thermal conductivity. Case 1 and Case 2 represents a fast change, either as an instant collapse in Case 1 or as a fast filling of air over some year as for Case 2. Case 3 represent a slower change based on the expected change for VIPs as building insulation (Simmler & Brunner 2005a). Case 4 has no change in thermal conductivity but the temperature in the return pipe decreased over time. This was the case for the field pipe DN 2\*80/250, and was investigated to find if this could influence the results of the method. The boundary temperatures were set to sinusoidal variations over the year.

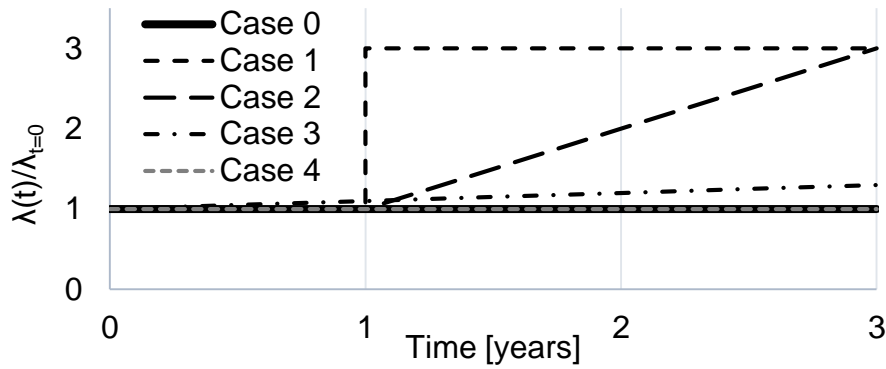


Figure 3.11: Description of how the thermal conductivity changes with time for the 5 simulation cases.

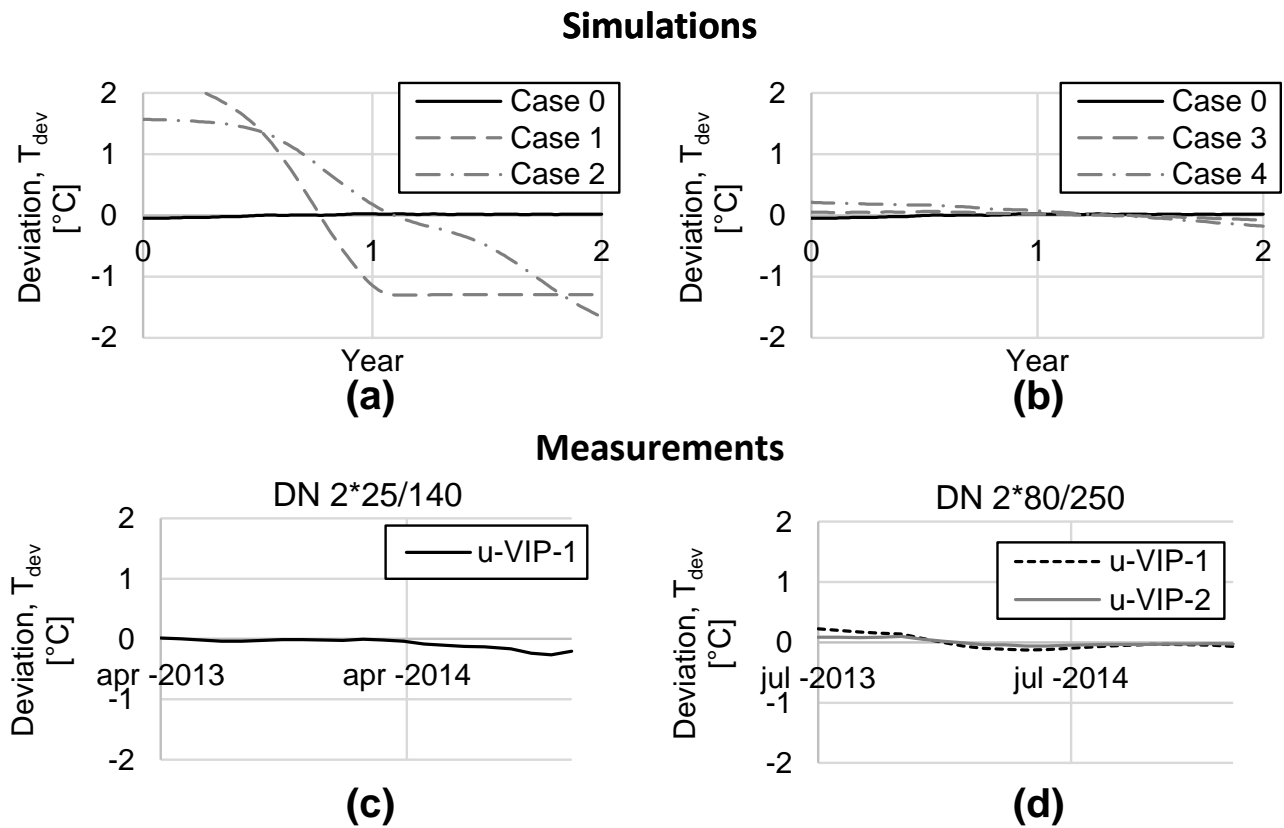


Figure 3.12: The resulting deviation between the superposition model and the results from measurements and simulations. The results from simulations are shown on top and the results from the measurements are shown at the bottom.

Paper **III** shows that the position between the supply and return pipe, u-VIP, had the smallest deviation between the superposition model and the field measurements. Therefore, u-VIP was chosen to use in the analysis. Paper **III** also show that a yearly average is needed to remove the influence from the temperature variation. The results for the deviation of a yearly average is shown in Figure 3.12. The deviation in the field measurements are much smaller than the

deviation in Case 1 and Case 2 which shows that no total collapse of the VIPs have occurred, they are still in good condition. From Case 3 and Case 4 it is shown that a sinking temperature in the return water would influence the model with a similar magnitude to a slower decrease in the thermal conductivity. This means that a slower deterioration of the panels cannot be detected by the model as it is.

# Chapter 4

## Nano-porous insulation in building walls

Nano-porous thermal insulation can be used to lower the heat loss from buildings, when used in place of conventional insulation types. Alternatively, the insulation can be used to decrease the thickness of the building walls. This creates challenges where a decreased thickness gives less space for structural elements in the building, also leading to a potentially larger thermal bridge effect.

For a building with a temporary high heat load, the optimum insulation performance varies. When heating is needed a low U-values is preferable and when cooling is needed a high U-value is preferable as long as the outdoor air is colder than the indoor air. This has been investigated theoretically by Hagentoft (2012) who shows that when the wall can change properties there is almost no need for temperature control by the HVAC system. Many concepts have been developed for adaptable façades, as presented by Loonen (2010), but few have been investigated in research projects. One way to adjust the U-value would be to change the pressure in the walls. Xenophou (1976) have patented a wall made up of cells which can be evacuated by a vacuum pump. The problem with such solution is that a high quality vacuum is needed and it is thus very sensitive to damages. Another concept is to have a metal hydride which can absorb and release hydrogen (Meister et al. 1997, Benson et al. 1994). Since hydrogen has very light molecules the thermal conductivity is high but when the hydrogen is adsorbed the thermal conductivity is considerably reduced. However, that kind of system would have to deal with the same challenge as for VIPs where the function would be ruined if air is permeated into the insulation.

Another method to create a variable U-value would be to use nano-porous insulation within a bag that can be evacuated and refilled. For nano-porous insulation a lower quality of vacuum is needed to change the thermal conductivity, compared to insulation with larger pores, as

presented in Chapter 2.

## 4.1 Wooden stud walls with aerogel blankets

Paper V investigates an aerogel blanket composite, where the aerogel is formed within a fiber mesh. The vapor diffusivity and the thermal conductivity was measured for the blanket and the results were used as input in wooden stud wall simulations.

The vapor diffusivity was measured with the wet cup method with relative humidity at 100% and 50% on on each side of the samples. The test were made for 3 samples each of two sizes. Two sizes were tested to eliminate any calculation error from the edges of the aerogel blankets where the fine porosity of the aerogel is disrupted. The vapor diffusivity was found to be  $5.5 \cdot 10^{-6} \text{ m}^2/\text{s}$  with a coefficient of variation of 6%, which is in the same range as an  $200 \text{ kg}/\text{m}^3$  mineral wool at  $8\text{-}12 \cdot 10^{-6} \text{ m}^2/\text{s}$  (Hagentoft 2005). No influence could be seen from the edges of the samples. The measurements were also compared to the diffusivity of a sample with a dust protection coating, which showed no influence on the diffusivity.

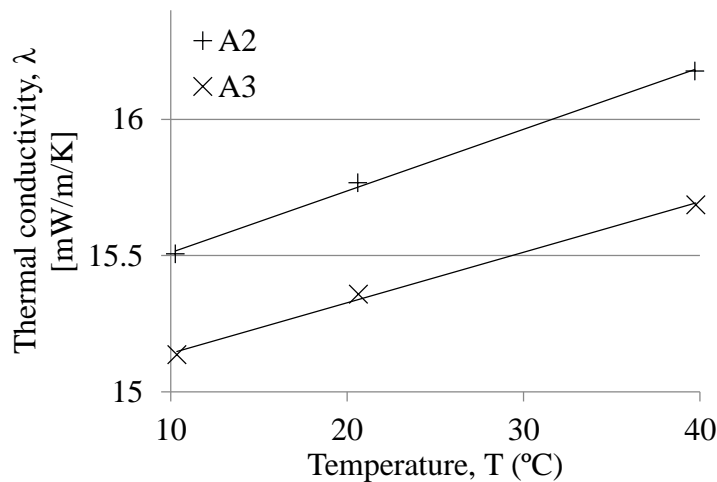


Figure 4.1: Relation between temperature and thermal conductivity for two samples of the aerogel blanket.

The thermal conductivity of the blanket was measured with a guarded heat flow apparatus. The relation between temperature and thermal conductivity is shown in Figure 4.1. The thermal conductivity changes with approximately  $0.02 \text{ mW}/\text{m}\cdot\text{K}$  per degree Celsius change in temperature. The thermal conductivity was also compared to the compression of the blankets since there had been indications that a compression would improve the thermal conductivity. The compression was measured as a change in sample thickness which correlates to the space given to the material in a wall assembly. The results are shown in Figure 4.2, where a 10% compression gives a decrease of around  $1 \text{ mW}/\text{m}\cdot\text{K}$ . It is important to note that the conductance,

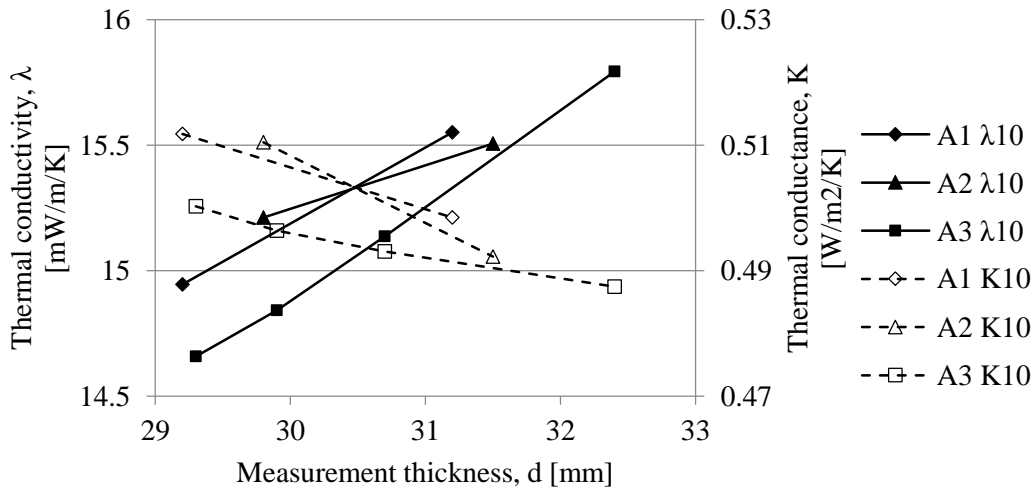


Figure 4.2: Relation between mechanical compression (measured as a thickness variation) and thermal conductivity for an aerogel blanket

related to the total heat flow through the material, increased. Compression will therefore lead to worse performance per cost for the material.

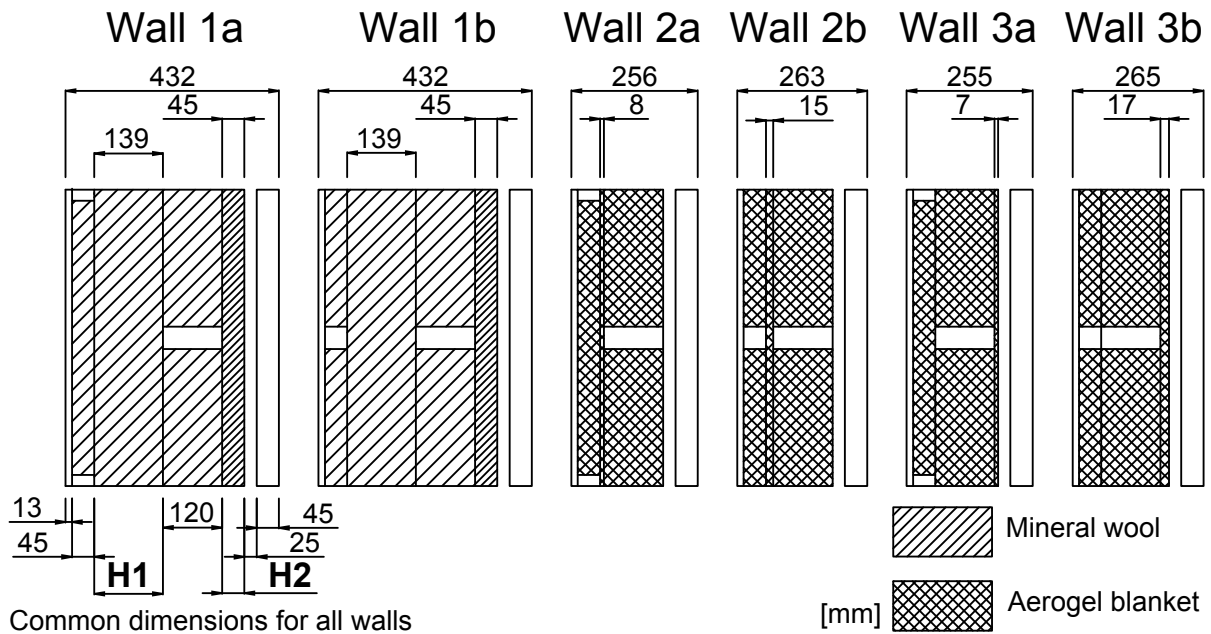


Figure 4.3: Description of the different walls used in the simulations. All walls have a simulated U-value of 0.10 W/m²K.

The results from the measurements were used in numerical heat and moisture simulations. Four aerogel blanket walls and two reference mineral wool walls were investigated, presented in Figure 4.3. The thermal performance was investigated using steady-state simulations in Comsol multiphysics (2015) and the thickness of the walls, the layers **H1** and **H2** in Figure 4.3, were adjusted until all walls had a U-value of 0.10 W/m²K. The aerogel walls, with less than half the thermal conductivity in the insulation, were around 40% thinner than the conventional walls.

The transient heat and moisture performance of the walls were simulated in Wufi2d (2015). The results were analyzed with the mold growth potential model by Hukka & Viitanen (1999). The results showed no greater risk of mold growth for an aerogel blanket compared to mineral wool. The only places where the model reached critical condition was in the air cavity of wall 2a and 2b, where it is close to outdoor conditions and no outer homogeneous insulation layer. Otherwise, the point where the outer wooden stud reach the service layer in the walls 2a and 3a has the highest mold growth potentials.

## 4.2 Effects from pressure changes in nano-porous insulation

In Paper VI the relation between the pressure and the thermal conductivity for an aerogel blanket and a fumed silica from a VIP has been investigated. The objective was to evaluate the potential to use a pressure change to vary the thermal conductivity in the insulation. The materials samples were put in a sealed plastic bag connected to a vacuum pump. The results from steady state measurements are shown in Figure 4.4. The performance as switchable insulation has been evaluated as a variation factor,  $\xi$  [-], defined as in Equation (4.1).

$$\xi = \frac{\lambda_{p.max}}{\lambda_{p.min}} \quad [-] \quad (4.1)$$

where  $\lambda_{p.max}$  [W/m·K] and  $\lambda_{p.min}$  [W/m·K] are the thermal conductivity at atmospheric pressure and at the minimal system pressure respectively. The variation factor was found to be around 1.5 for the aerogel blanket and 2.6 for the fumed silica. This means that the fumed silica can create a larger variation in the U-value of a wall. One reason for the results is that the aerogel has a very low thermal conductivity already at atmospheric pressure. It should be noted that neither of the materials were optimized for this kind of application.

The transient effects of a pressure change was also investigated. The thermal conductivity of the samples of fumed silica and aerogel blankets was measured while the pressure was changed. For an ideal situation, where the thermal conductivity of a material is changed instantly, the heat flow measured through the material would change instantly as well. But, when air is evacuated, the change is not instant but rather a diffusion process. At the same time, various other effects might influence the measurement.

The presented varied thermal conductivity is a representative measurement calculated from the heat flow. When the transient effects are taken into consideration it is important to know how the heat flow meter is positioned. In these measurements it is placed on the cold side of

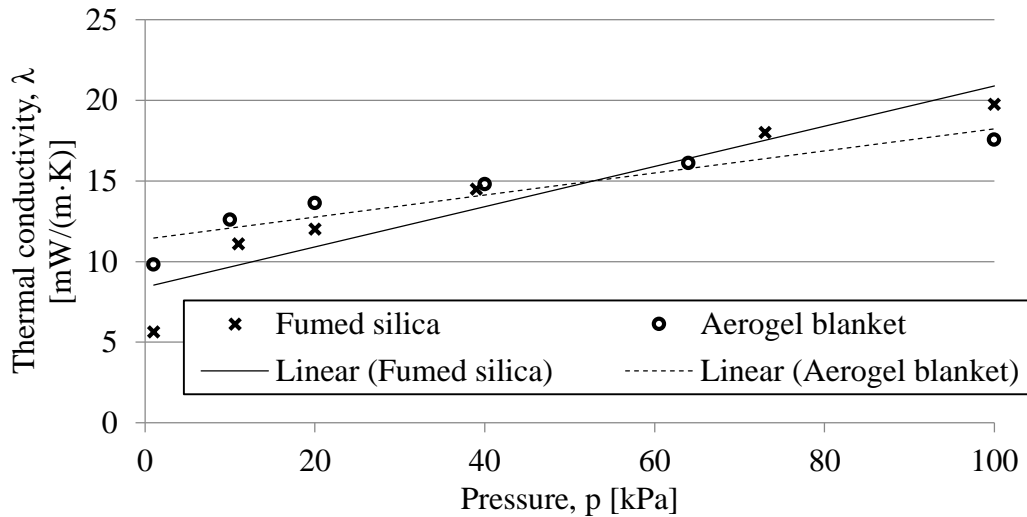


Figure 4.4: Relation between pressure and thermal conductivity for a fumed silica and an aerogel blanket

the sample which means that an increase in the sample temperature would be registered as an increased thermal conductivity and opposite for a decrease in temperature.

The resulting thermal conductivity is shown in Figure 4.5 for the fumed silica and in Figure 4.6 for the aerogel blanket. The change of the thermal conductivity can be divided into two parts: the slow change towards a steady state value and some local peak effects at the moment of the pressure change. It should be noted that the time scale varies between the different materials. The fumed silica took much longer time before reaching equilibrium compared to the aerogel blanket. On the other hand, the main change in thermal conductivity happened quite fast for both materials.

Four mechanisms have been found which could explain the behavior of the thermal conductivity measurement presented in Figure 4.5 and Figure 4.6 :

- When evacuating or refilling with air, there might be a delay before the air molecules have been evenly spread throughout the pore system.
- When the pressure is changed, thermodynamic processes will change the temperature. With an increased pressure, the temperature increases and with a decrease in pressure the temperature decreases.
- When the sample is filled with air from the surrounding room, the air will be of a certain temperature. This air will influence the temperature of the sample.
- In the heat flow meter apparatus used in the measurements, a small resistance has been detected between the regulated temperature and the plate temperature. With an extra

resistance the temperature gradient in the material will be changed and thereby, another steady state will be formed.

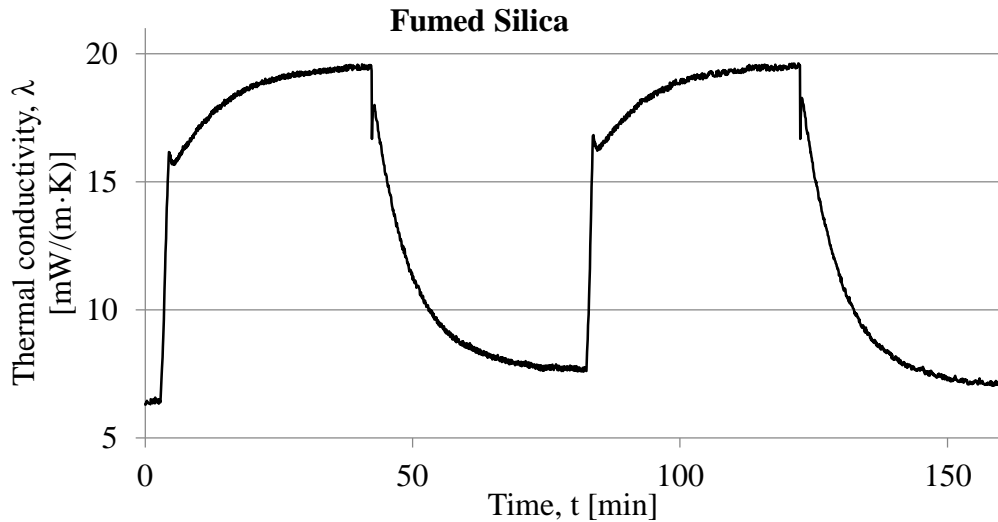


Figure 4.5: Measured thermal conductivity of a fumed silica at a varied pressure. The pressured was cycled between 2 kPa and atmospheric pressure at 40 min intervalls.

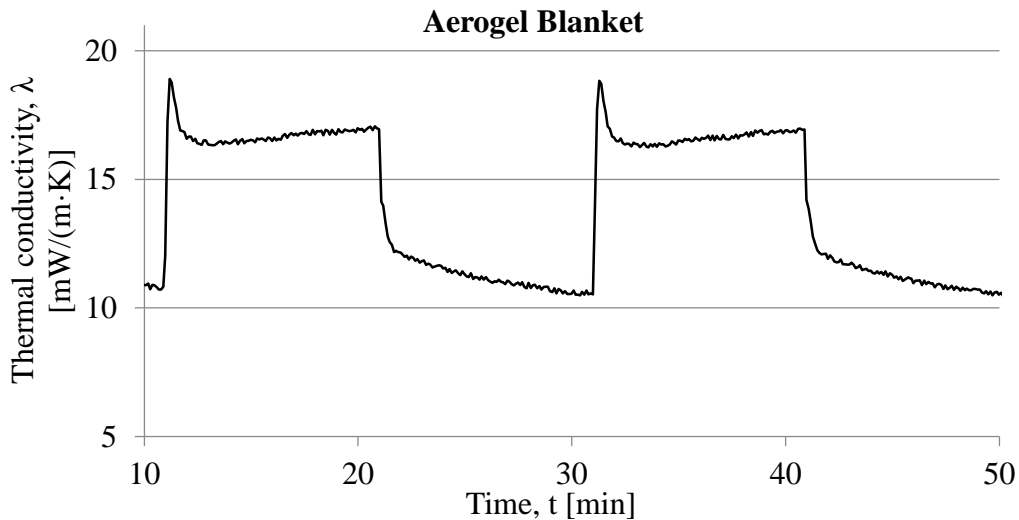


Figure 4.6: Measured thermal conductivity of an aerogel blanket at a varied pressure. The pressured was cycled between 2 kPa and atmospheric pressure at 20 min intervalls.

These mechanisms were investigated through one dimensional finite volume simulations in Matlab (2015). The sample was divided into 10 cells between a constant temperature boundary and a thermal resistance boundary. The effect from intrusion of air, with room temperature, was modeled according to Equation (4.2), the thermodynamic effect of pressure change was modeled according to Equation (4.3) and the diffusion of gas into the pores were modeled as in Equation (4.4).

$$T_{t+1}(x) = T_{room} \cdot \frac{C_a}{C_a + C_m} + T_t(x) \cdot \frac{C_m}{C_a + C_m} \quad (4.2)$$

$$T_{t+1}(x) = T_t(x) + \Delta T_{therm} \quad (4.3)$$

$$P_{t+1} = P_t + D \cdot (P_t - P_{out}) \cdot \Delta t \quad (4.4)$$

where  $T_{t+1}$  and  $T_t$  are the temperatures before and after the change,  $T_{room}$  is the room temperature,  $C_a$  and  $C_m$  are the volumetric heat capacity of the air and the solid material respectively and  $\Delta T_{therm}$  is the temperature difference created by a pressure change in the gas. The temperatures  $T_{room}$  and  $\Delta T_{therm}$  were 24.2°C and 0.5°C respectively and were obtained by temperature measurements with thermocouples positioned in the room air and in the center of the sample during measurement. The pressures  $P_{t+1}$  and  $P_t$  are before and after the time step,  $P_{out}$  is the imposed pressure cycling between a maximum and a minimum,  $D$  is a diffusion term and  $\Delta t$  is the time step length. The thermal conductivity of the sample was then defined as linearly dependent on the pressure, varying between a maximum thermal conductivity and a minimum thermal conductivity at the maximum and minimum pressures respectively. The thermal resistance was modeled as a boundary resistance without mass between the regulated temperature and the first cell on the cold side.

The result from the simulations are shown in Figure 4.7 for the fumed silica sample. The results can be compared to the measurements on fumed silica in Figure 4.5. The results show very good resemblance for the evacuation part. The air filling seems to be a faster process in the real case than in the simulation. When evacuating, a vacuum pump was used and when refilling, the valves were opened. At the instant of the pressure change the thermodynamic effect and the room air temperature have a large influence on the results, but after some time the diffusion takes over and dominates completely.

### 4.3 Building simulations on building with switchable insulation

An energy balance was made for a office building in Paper VII to assess the potential impact of a switchable insulation made from a nano-porous insulation material. The variation factor,  $\xi$ , was chosen to 3 based on the fumed silica. The energy balance at every hour,  $Q_{balance}$  [W], is shown in Equation (4.5):

$$Q_{balance}(t) = Q_{int}(t) + Q_{sol}(t) \cdot g - K(t) \cdot (T_i(t) - T_e(t)) \quad (4.5)$$

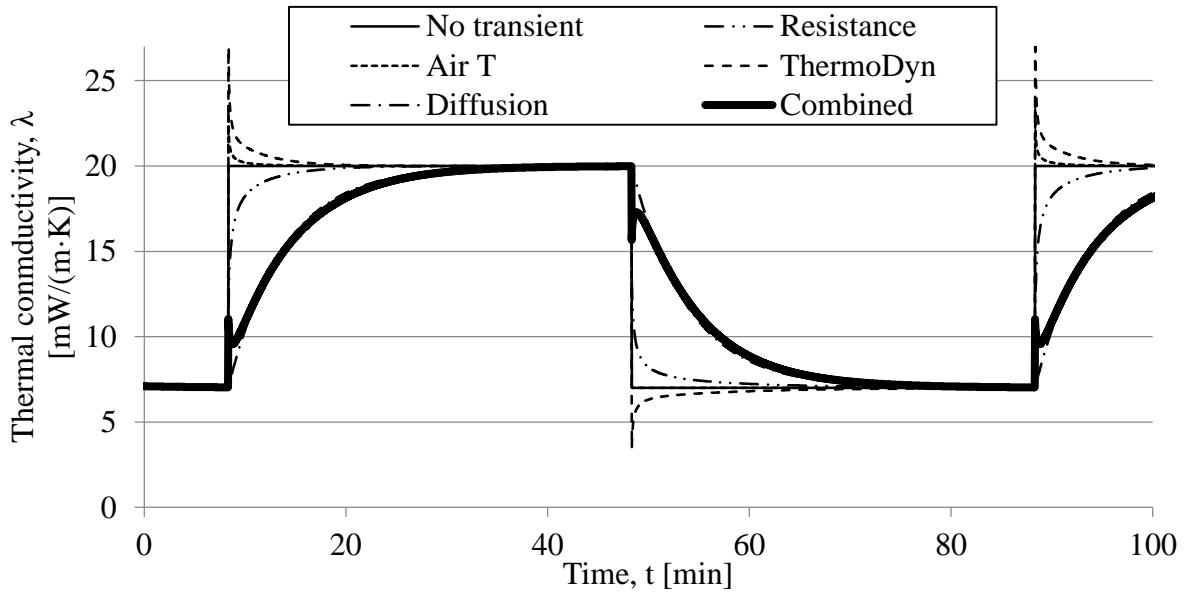


Figure 4.7: Simulated change in thermal conductivity of a fumed silica at varying pressure. The pressure was changed between 2 kPa and 100 kPa at 40 min intervals. The figure show the consequence of different transient effects. The curve for diffusion is almost completely covered by the combined result

where  $Q_{int}$  [W] is the internal heat load,  $Q_{sol}$  [W] is the solar heat load on the windows,  $g$  [-] is the solar transmittance through the windows and  $T_i$  and  $T_e$  [°C] is the interior and the exterior temperatures, all at the time  $t$ . The term  $K$  [W/K] is the total thermal conductance through the building envelope for which the transmission parts (the U-values) were varied with a variation factor  $\xi$  to minimize  $Q_{balance}$ . The internal loads were taken from Boverket (2007) and hourly weather data from Göteborg was used. The input of the simulations are described more in detail in Paper VII.

The results from the simulations are shown in Figure 4.8 as the energy use as a function of the U-value. Figure 4.8 (a) compares heating and cooling for a variation factor,  $\xi$ , of 1, corresponding to no variation, and 3. The results indicate that a lower U-value is preferable which diminishes the effect of the variation. Often, energy used for cooling is considered to be worse than energy used for heating based on the source of primary energy. A weighting factor  $W$  was multiplied to the cooling loads. The result on the total weighted energy use for the weighting factors 1, 2 and 3 are presented in Figure 4.8 (b). The minimum values are marked with an X. With a weighting factor of 1, a lower U-value is better and the influence of the variation is small. With a higher weighting factor, the difference in total energy use increases between the building with variable U-value and the building without. More importantly, with a variable U-value, the optimum minimum U-value is shifted to a considerably higher value. This correspond to thinner wall constructions with less material needed.

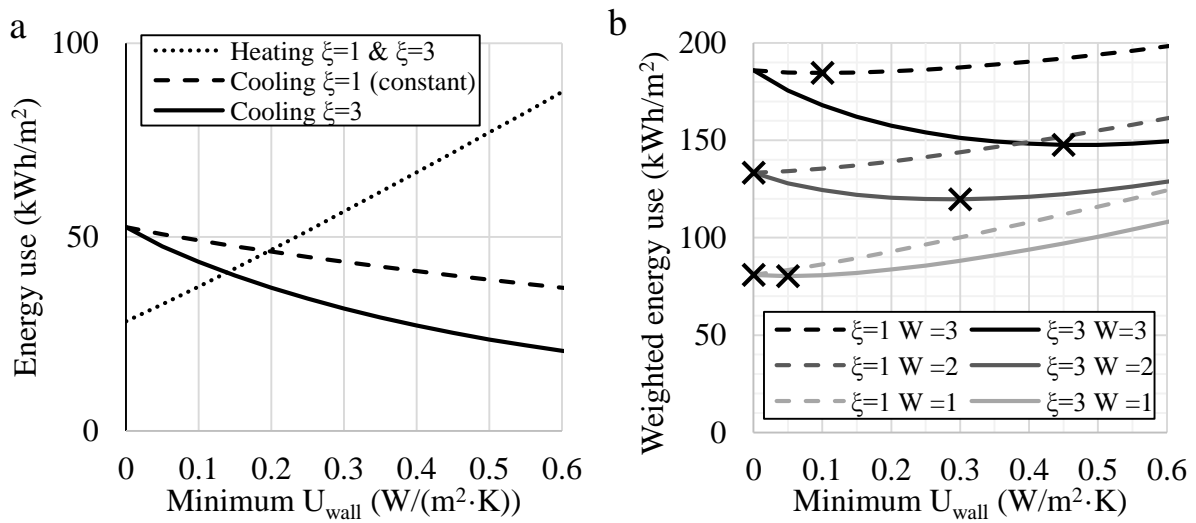


Figure 4.8: Effect of a variable U-value in an office building. In (a) the heating is compared to the cooling and in (since the minimum U-value have been used as baseline for the variation, the heating energy use is independent of the variation) (b) different weighting factors for the weighted relation between cooling energy and heating energy is presented.

# Chapter 5

## Conclusion

This thesis has been divided into two main themes: hybrid insulation district heating pipes and nano-porous insulation in building walls. It is shown that the use of VIPs in district heating pipes is a plausible method to reduce the heat losses from the pipes without increasing their thickness. The results for the investigated wall solutions are further from implementation but the studies indicate some possible positive effects. The main conclusions of the thesis are:

- When VIPs are used in hybrid insulation district heating pipes, a reduction of the heat losses in the range of 30% can be expected when compared to conventional pipes of the same dimension. For the supply pipe heat losses of twin pipes, the improvement is even higher, up to around 50%, at a cost of an increase in the return pipe losses.
- How the thermal bridges of the VIP are positioned in a twin pipe has a large influence on the thermal performance. With a high thermal conductivity in the vacuum envelop, the variation is 20% between the best and the worst position. The position of the outer edge of the overlap was shown to be crucial for the thermal performance.
- After three years of field measurements on pipes connected to a district heating network with temperatures up to 90°C, there is yet no sign of a collapse of the VIPs. A superposition model has been developed to evaluate the deterioration of the VIPs. The model showed that a slow deterioration cannot be ruled out, but the model could not differentiate it from other variations in the system.
- When aerogel blankets were investigated for use in load bearing wooden stud walls with a U-value of 0.1 W/m<sup>2</sup>K, the thickness could be reduced by 40%. Furthermore, the effect of the thermal bridge through the studs increase with thinner walls. Numerical simulations also showed that the thermal bridge of the studs, in the thinner aerogel walls, could create a higher risk of mold growth inside the wall.

- Measurements of the thermal conductivity was made on a fumed silica sample and an aerogel blanket sample at different pressures. The variation between the thermal conductivity at atmospheric pressure and the minimum pressure (around 1 kPa), were in the size range of 1.5 for the aerogel blanket and 3 for the fumed silica.
- When the pressure was varied in a fumed silica sample and an aerogel blanket sample, five effects were investigated to see how they influenced the measurements. In a short time perspective, the change in temperature from pumping in air and changing the pressure seemed to dominate the change in heat flow. In a longer time perspective some kind of diffusion process seemed to dominate.
- The simulations of energy use in an office building indicated that, in a cold climate, a lower U-value is more important than a variable U-value for the tested magnitude of variation factors. When cooling was weighted as more energy demanding than heating the benefit of variability increased. Moreover, for this case, the optimal U-value of the walls increased, meaning thinner walls were more beneficial.

# Chapter 6

## Future work

The concepts for using nano-porous thermal insulation, presented in this thesis, demand more research before they can be implemented. Some suggestions for the next step of the research is presented here.

Hybrid insulation district heating pipes:

- The durability of the VIPs at district heating temperature have to be more thoroughly investigated to be able to guarantee their service life. Long time/high temperature tests of hybrid insulation pipes have already been initiated. The pipes have been mounted in a rig where hot oil is circulated through the service pipe and the temperature on the back of the panels have been measured continuously. The measurements have been running for approximately 3 years and the results need an in depth analysis.
- The high temperature measurements can be complemented by the ongoing field measurements. So far they have been registering the temperatures for more than 3 years. As long as the measurements are active they will give continuous information of the panels long term performance.
- At the, moment every new measurement on district heating pipes with VIPs have been using the latest development of the panels, few measurements have used the same panels. To get knowledge of the average thermal performance and the variation, more samples need to be measured for a statistical analysis.
- The results from the simulations can be used to show th e prospect of the technology. To use it for more exact design it would have to be validated against measurements. The effect of the thermal bridges through the envelope of the VIPs could be measured from carefully planned laboratory measurements on pipes with a well known layout.

- It would be useful to be able to assess the performance of the VIPs with one single measurement, instead of using long time continuous measurements. Therefore, there is a need to investigate new potential technology for performance measurements.

Nano-porous insulation in building walls:

- For variable insulation, the magnitude of the variation factor is the central property. This thesis presents measurements on two materials which are already in production. It would be interesting to try to make a theoretical investigation of the largest possible variation factor that could be obtained for pressure regulated nano-porous insulation. This could give information on what kind of material to try to produce and show the potential limits of the concept.
- The presented measurements have all been on material level. A natural next step would be to try and develop a solution on component level. A component would add some extra layers of complexity which could influence the performance, such as thermal bridges.
- One crucial point of the variable insulation system is the energy needed to pump out air, both to evacuate the panels and also to keep them evacuated. The optimal relation between the system diffusion tightness and needed pump energy would have to be investigated.
- If further research on variable insulation show promise, it would be necessary to investigate it in a building system. A variety of different properties would have to be tested, such as: acoustics and durability of the diffusion barrier.

# Bibliography

- Araki, K., Kamoto, D. & Matsuoka, S. (2009), ‘Optimization about multilayer laminated film and getter device materials of vacuum insulation panel for using at high temperature’, *Journal of Materials Processing Technology* **209**(1), 271 – 282.
- Baetens, R., Jelle, B. & Gustavsen, A. (2010a), ‘Aerogel insulation for building applications: A state-of-the-art review’, *Energy and Buildings* **43**, 761–769.
- Benson, D. K., Potter, T. F. & Tracy, C. E. (1994), Design of a variable-conductance vacuum insulation, Technical report, SAE Technical Paper.
- Bøhm, B. (2001), ‘Experimental Determination of Heat Losses from Buried District Heating Pipes in Normal Operation’, *Heat Transfer Engineering* **22**(3), 41–51.
- Bøhm, B. & Kristjansson, H. (2005), ‘Single, twin and triple buried heating pipes: on potential savings in heat losses and costs’, *International Journal of Energy Research* **29**(14), 1301–1312.
- Boverket (2007), *Indata för energiberäkningar i kontor och småhus, en sammanställning av brukarrelaterad indata för elanvändning, personvärme och tappvarmvatten.*, Boverket, Karlskrona.
- Brunner, S. & Simmler, H. (2008), ‘In situ performance assessment of vacuum insulation panels in a flat roof construction’, *Vacuum* **82**(7), 700–707.
- Caps, R. & Fricke, J. (2000), ‘Thermal conductivity of opacified powder filler materials for vacuum Insulations’, *International Journal of Thermophysics* **21**(2), 445–452.
- Comsol multiphysics (2015), ‘COMSOL Multiphysics Modeling Software’.  
**URL:** [www.comsol.com](http://www.comsol.com)
- Dalla Rosa, A., Li, H. & Svendsen, S. (2011), ‘Method for optimal design of pipes for low-energy district heating, with focus on heat losses’, *Energy* **36**(5), 2407–2418.
- Ebert, H.-P. (2011), Thermal properties of aerogel, in ‘Aerogels Handbook’, Springer New York, New York, NY, pp. 537 – 563.
- Fricke, J., Lu, X., Wang, P., Büttner, D. & Heinemann, U. (1992), ‘Optimization of monolithic silica aerogel insulants’, *International journal of heat and mass transfer* **35**(9), 2305–2309.
- Ghazi Wakili, K., Bundi, R. & Binder, B. (2004), ‘Effective thermal conductivity of vacuum insulation panels’, *Building Research & Information* **32**(4), 293–299.
- Ghazi Wakili, K., Stahl, T. & Brunner, S. (2011), ‘Effective thermal conductivity of a staggered double layer of vacuum insulation panels’, *Energy and Buildings* **43**(6), 1241–1246.

- Haavi, T., Jelle, B. P. & Gustavsen, A. (2012), ‘Vacuum insulation panels in wood frame wall constructions with different stud profiles’, *Journal of Building Physics* **36**(2), 212–226.
- Hagentoft, C.-E. (2005), *Introduction to building physics*, Studentlitteratur, Lund, Sweden.
- Hagentoft, C.-E. (2012), Potential impact on innovative and active building envelope components and materials, in ‘Proceedings of the 5th IBPC’, Kyoto, Japan, pp. 309–315.
- Hukka, E. & Viitanen, H. (1999), ‘A mathematical model of mould growth on wooden material’, *Wood Science and Technology* **33**.
- Hümmer, E., Rettelbach, T., Lu, X. & Fricke, J. (1993), ‘Opacified silica aerogel’, *Thermochimica Acta* **218**, 269–276.
- Johansson, P., Hagentoft, C.-E. & Sasic Kalagasidis, A. (2014), ‘Retrofitting of a listed brick and wood building using vacuum insulation panels on the exterior of the facade: Measurements and simulations’, *Energy and Buildings* **73**, 92–104.
- Kistler, S. S. (1931), ‘Coherent expanded aerogels and jellies’, *Nature* **127**, 741.
- Kistler, S. S. & Caldwell, A. G. (1934), ‘Thermal conductivity of aerogels’, *Journal of Industrial and Engineering Chemistry* **26**(6), 658–662.
- Loonen, R. (2010), Climate Adaptive Building Shells, Master of science thesis, TU Eindhoven, Eindhoven, Netherlands.
- Matlab (2015), ‘Matlab’.  
**URL:** <http://se.mathworks.com/products/matlab/>
- Meister, M., Horn, R., Hetfleisch, J., Caps, R. & Fricke, J. (1997), Switchable thermal insulation for solar heating, in ‘Thermal conductivity 24/Thermal Expansion 12’, Technomic Publishing Company Inc., Lancaster, USA, pp. 417–427.
- Nilsson, O., Fransson, A. & Sandberg, O. (1986), Thermal properties of silica aerogel, in ‘Aerogels’, number 6 in ‘Springer Proceedings in Physics’, Springer-Verlag, Berlin, pp. 121–132.
- Pietruszka, B., Babinska, J. & Gerylo, R. (2012), Aerogel-based thermal insulation materials - structure and properties, in ‘Proceedings of the 5th IBPC’, Kyoto, pp. 117–123.
- Pietruszka, B. & Gerylo, R. (2010), Implementation of nanoporous thermal insulations to improve the energy efficiency of curtain walling structures, in ‘Proceedings of the 10th international conference on modern building materials, structures and techniques’, Vilnius Gediminas Technical University, Lithuania, pp. 255–258.
- Reidhav, C. & Werner, S. (2008), ‘Profitability of sparse district heating’, *Applied Energy* **85**(9), 867–877.
- Reim, M., Körner, W., Manara, J., Korder, S., Arduini-Schuster, M., Ebert, H.-P. & Fricke, J. (2005), ‘Silica aerogel granulate material for thermal insulation and daylighting’, *Solar Energy* **79**(2), 131 – 139. {CISBAT} 03: Innovation in Building Envelopes and Environmental Systems.

- Reim, M., Reichenauer, G., Körner, W., Manara, J., Arduini-Schuster, M., Korder, S., Beck, A. & Fricke, J. (2004), 'Silica-aerogel granulate: Structural, optical and thermal properties', *Journal of non-crystalline solids* **350**, 358–363.
- Rubin, M. & Lampert, C. (1983), 'Transparent silica aerogels for window insulation', *Solar Energy Materials* **7**(4), 393–400.
- Scheuerpflug, P., Caps, R., Buttner, D. & Fricke, J. (1985), 'Apparent thermal conductivity of evacuated SiO<sub>2</sub>-aerogel tiles under variation of radiative boundary conditions', *International journal of heat and mass transfer* **28**(12), 2299–2306.
- Schreiber, E., Boy, E. & Bertsch, K. (1986), Aerogel as a transparent thermal insulation material for buildings, in 'Aerogels', number 6 in 'Springer Proceedings in Physics', Springer-Verlag, Berlin, pp. 133–139.
- Schwab, H., Heinemann, U., Beck, A., Ebert, H.-P. & Fricke, J. (2005), 'Permeation of Different Gases Through Foils used as Envelopes for Vacuum Insulation Panels', *Journal of Building Physics* **28**(4), 293–317.
- Simmler, H. & Brunner, S. (2005a), 'Vacuum insulation panels for building application', *Energy and Buildings* **37**(11), 1122–1131.
- Simmler, H., Brunner, S., Heinemann, U., Schwab, H., Kumaran, K., Qunard, D., Sallée, H., Noller, K., Küçükpinar-Niarchos, E., Stramm, C., Tenpierik, M., Cauberg, H. & Erb, M. (2005b), Study on VIP-components and Panels for Service Life Prediction of VIP in Building Applications (Subtask A), Technical report, IEA/ECBCS Annex 39.
- Spagnol, S., Lartigue, B., Trombe, A. & Despetis, F. (2009), 'Experimental Investigations on the Thermal Conductivity of Silica Aerogels by a Guarded Thin-Film-Heater Method', *Journal of Heat Transfer* **131**(7), 074501.
- Sprengard, C. & Holm, A. H. (2014), 'Numerical examination of thermal bridging effects at the edges of vacuum-insulation-panels (VIP) in various constructions', *Energy and Buildings* **85**, 638–643.
- SS-EN 253 (2009), District heating pipes - Preinsulated bonded pipe systems for directly buried hot water networks - Pipe assembly of steel service pipe, polyurethane thermal insulation and outer casing of polyethylene, Standard 253:2009, Swedish standards institute.
- Statistics Sweden (2013), El-, gas- och fjärrvärmeförsörjningen 2013. Slutlig statistik, Technical Report SM1401.
- Svendsen, S. (1992), 'Solar collector with monolithic silica aerogel', *Journal of non-crystalline solids* **145**, 240–243.
- Tamon, H., Sone, T. & Okazaki, M. (1997), 'Control of Mesoporous Structure of Silica Aerogel Prepared from TMOS', *Journal of Colloid and Interface Science* **188**(1), 162–167.
- Tenpierik, M. & Cauberg, H. (2007), 'Analytical Models for Calculating Thermal Bridge Effects Caused by Thin High Barrier Envelopes around Vacuum Insulation Panels', *Journal of Building Physics* **30**(3), 185–215.

- Tillotson, T. M. & Hrubesh, L. W. (1992), ‘Transparent Ultralow-density silica aerogels prepared by a two-step sol-gel process’, *Journal of non-crystalline solids* **145**, 44–50.
- Wallentén, P. (1991), Steady-State heat loss from insulated pipes, Technical Report TVBH-3017, Lund Institute of Technology, Lund, Sweden.
- Willems, W., Schild, K. & Hellinger, G. (2005), Numerical investigation on thermal bridge effects in vacuum insulating elements, *in* ‘7th international vacuum insulation symposium’, Zurich, Switzerland.
- Wufi2d (2015), ‘Wufi 2d’.  
**URL:** <https://wufi.de/en>
- Xenophou, T. (1976), ‘System of using vacuum for controlling heat transfer in building structures, motor vehicles and the like’.
- Zinko, H., Bøhm, B., Ottosson, U., Rämä, M. & Sipilä, K. (2008), District heating in areas with low heat demand density, Technical Report 8DHC-08-03, IEA-DHC.